ADDIS ABABA UNIVERSITY

ADDIS ABABA INSTITUTE OF TECHNOLOGY

SCHOOL OF CIVIL AND ENVIRONMENTAL ENGINEERING

SEISMIC PERFORMANCE ASSESSMENT OF SHEAR CRITICAL REINFORCED CONCRETE FRAME STRUCTURES

A Thesis in Structural Engineering

By Nahom Worku

GSR/3639/11

October, 2024

Addis Ababa

A Thesis

Submitted in Partial Fulfillment of the Requirements for the Degree of Master of Science

The undersigned have examined the thesis entitled '**Seismic Performance Assessment of Shear Critical Reinforced Concrete Frame Structures**' presented by **NAHOM WORKU**, a candidate for the degree of **Master of Science** and hereby certify that it is worthy of acceptance.

Dr. Ing. Adil Zekaria	for Esayas.	Feb-11-2025
Advisor	Signature	Date
Dr. Esayas Gebreyouhannes	Esayas.	Feb-11-2025
Internal Examiner	Signature	Date
Prof. Girma Zerayohannes	for	Feb. 12/2025
External Examiner	Signature	Date
Dr. Abraham Gebre	Abrham Gebre (Dr.) Dean, School of Civil & Environmental Engineering	
Chair person	Signature	Date

Director of Postgraduate Program
Addis Ababa University
Addis Ababa Institute of Technology

UNDERTAKING

I certify that research work titled “enter title of your research proposal here” is my own work. The work has not been presented elsewhere for assessment. Where material has been used from other sources it has been properly acknowledged / referred.

Signature of Student

Nahom Worku

ABSTRACT

A substantial number of currently operating buildings are built as per requirements of older codes that are without proper seismic provisions that ensure ductility. These structures may be susceptible to exhibit a catastrophic shear failure if an important seismic load is imposed. However, most analyses of reinforced concrete frames commonly ignore shear effects. This simplification may lead to significant errors and may result in severely unconservative and unsafe calculation of strength and ductility.

In this study the seismic performance of a shear critical frame was investigated through finite element analysis using Vector 2, Seismostruct and ETABS. After the analyses the results were examined using experimental data from a laboratory test carried by Kien Vinh Duong, Shamim A. Sheikh, and Frank J. Vecchio at the University of Toronto. The accuracy of various finite element software in predicting shear critical behavior was scrutinized. Finaly a proposal for steps to be followed to improve the results of one of the most commonly used structural analysis software was set forth, and its outputs were verified against experimental data.

The results show the difficulties in seismic performance assessment of shear critical structures, particularly while using the widely used commercial structural analysis software. The educational and speciality software, namely Vector 2 and Seismostruct, gave more accurate results. The widely used software required the foresight to predict possible shear critical failure of the structure. This indicates that the standard user might get a misleading result if not aware of possible shear critical mechanism. A proposal was set forth for the performance assessment of shear critical structures for practitioners utilizing a widely use software, ETABS. The proposal describes the details followed in generating accurate user defined shear hinges with the aid of a free supportive software. Results show that the steps proposed showed a considerable improvement in the accuracy of the finite element analysis when compared to experimental data.

Keywords: nonlinear analysis; pushover; shear; shear hinge; reinforced concrete; frame structure; fiber model; Vector 2; Seismostruct; ETABS;

ACKNOWLEDGMENTS

First of all, I would like to thank God for giving me the strength and the patience to complete this thesis paper.

My next appreciation goes to my advisor, Dr. Ing. Adil Zekaria for always being there when I needed his support and for pushing me to do a better job. His advice was very constructive and motivational, which guided me through my time of research and writing of this thesis.

I would like to express my heartfelt appreciation to Dr. Esayas Gebreyouhannes, who gave valuable insight and knowledge that aided this research immensely and for always being there when I needed his support.

I sincerely would also like to thank Dr. Abraham Gebre for his encouragement and inspiration that helped me to push through my work on this thesis, despite of many difficulties.

Last but not the least, I would like to express my deepest gratitude to my family for providing me continuous support and encouragement throughout my years of study and through the process of researching. A special heartfelt gratitude goes to my mother Sis. Yeshareg Abate for always believing in me and providing unconditional support throughout my study. This accomplishment would not have been possible without them.

TABLE OF CONTENTS

LIST OF TABLES

LIST OF FIGURES

LIST OF SYMBOLS

A_s	Area of tensile longitudinal steel reinforcement
d	Longitudinal tension reinforcement
d_b	Diameter of reinforcing bar
Es	Initial tangent stiffness of reinforcement
E_c	Initial tangent stiffness of concrete
G_c	Shear modulus of Elasticity of concrete
$[B]$	Element strain-displacement matrix
$[D]$	Composite material stiffness matrix
$[K]$	Element stiffness matrix
ΔY	Yield Displacement
ε_{ci}	Compressive principal strain
ε_p	Concrete compressive strain corresponding to f_p
ε_{sh}	Reinforcement strain at onset of strain hardening
ε_u	Ultimate strain of reinforcement
ε_0	Concrete compressive strain corresponding to $f_c^{'}$
$f_c^{'}$	Concrete cylinder uniaxial compressive strength
f_{ci}	Principal compressive stress
f_{ci}^b	Descending branch principal compressive stress
f_{lat}	Summation of principal stresses, acting transversely
f_p	peak concrete compressive stress
n	curve fitting parameter
γ	shear strain

ϕ	Rotation
ψ	Curvature
μ	poisons ratio

LIST OF ABBREVIATIONS

FE	Finite element
CQC	Complete quadratic combination
SRSS	Square root of sum of squares
LVDT	Linear Variable Differential Transformer
DCL	Ductility class low
DCM	Ductility class medium
CFRP	Carbon Fiber-Reinforced Polymer
IO	Immediate occupancy
LS	Life safety
CP	Collapse prevention

CHAPTER 1 INTRODUCTION

1.1 Background of the study

Although today's design codes often require structures to be constructed with a ductile character, many concrete frame structures constructed prior these modern codes were built based on practices that are considered inadequate today. Performance assessment of such structure is required to ensure their safety for continued usage.

The need to assess performance of existing structures is fast growing in Ethiopia since revised Ethiopian building code (ES EN1998:2015) shows a major change on the expected peak ground acceleration for major cities including the capital, Addis Ababa. For the past several years large numbers of buildings are designed and constructed using the previous building code, it becomes imperative to conduct a performance assessment on these structures using provisions of revised code. [20]

The most common and practical way of assessing the performance of existing structures is a static nonlinear pushover analysis. Pushover analysis evaluates structural requirements by estimating the forces and deformations required during an earthquake through static inelastic analysis and compares these requirements with the available capacity for the performance level. This analysis is based on the analysis of key factors including global and inter story drifts, nonlinear member deformations, material stresses , and the state of joints and connections.

A pushover analysis evaluates the expected performance of a structural system by estimating its strength and deformation demands in design earthquakes by means of static inelastic analysis and comparing these demands to available capacities at the performance levels of interest. The evaluation is based on an assessment of important parameters, including global drift, inter story drift, inelastic element deformations, deformation between elements, and element and connection forces. [9]

The concept of ductility and ductile detailing rule are part and parcel of most modern building codes including our own ES-EN-2015. These modern Building Codes prescribe detailed seismic design guidelines that encompass a wide range of requirements, such as detailing requirements, ductility requirements, and detailed steps on the derivation of the earthquake demand. However, for existing structures that were not subject to such guidelines making the common approach of performance analysis using ductile failure mode assumptions questionable.

A reinforced concrete frame structure built to older codes may lack proper seismic design which may lead to undesirable situations like: insufficient amount of transverse reinforcement, inadequate location and insufficient length for lap splices of longitudinal reinforcement, insufficient embedment length for longitudinal reinforcement, lack of strong column/weak beam design approach. The aforementioned issues may lead to inability of the structure to develop its structural full flexural capacity, and, may lead to a non-ductile behavior.[3]

A substantial number of currently operating buildings are built without properly seismic provisions as per older codes, and may be susceptible to exhibit a shear failure if an important seismic load is imposed. It becomes necessary to conduct performance assessment on those structures according to present seismic knowledge in order to determine their capacity and take corrective measures if needed. For the particular case of shear critical reinforced concrete structures, an accurate seismic assessment is not as simple as the flexural-critical situation.

In most analyses of reinforced concrete frames, it is common to ignore shear effects. However, there are cases where this simplification may lead to significant errors. These may be apparent for frames with high depth to span ratio where shear deformation is significant. It is also incorrect to neglect shear effects if the design was not done up to modern codes which ensure ductile behavior. Not considering shear effects for these types of structures results in a misleading and unsafe prediction of strength and ductility.

Furthermore, most of the commercially available FE software ignore shear effects by default which may mis lead practitioners. While this software may allow the use of shear hinges if such failure is anticipated by the user, definition of the user shear hinge requires expert knowledge of shear behavior or the access and use of specialized supporting software.

This research will focus on performance assessment without neglecting the role of shear effects. Finite element analyses will be conducted using commonly used commercial, specialized commercial and educational software. This will help examine the gaps in widely used commercial software and the general approach used by practicing professionals when it comes to performance assessment of shear critical frames.

1.2 Statement of the Problem

Flexural and shear failures are two most common failure modes that can happen in reinforced concrete frame sections. While structures failing in flexure has been studied well and their seismic performance can be estimated with great accuracy the same cannot be said of shear critical structures. This can be attributed to the complex nature of shear behavior. This can be further exemplified by the fact most commercially available finite element software have difficulty when trying to predict shear critical behavior.

1.3 Objectives of the study

1.3.1 General objectives

The objective of the research is to understand and predict the behavior of shear critical reinforced concrete frames under seismic actions using nonlinear finite element analyses, and in doing so to assess the capability and ease of various FE software when it comes to estimating shear critical behavior.

1.3.2 Specific objectives

The specific objectives of this study can be summarized as follows:

i. To perform and validate a static non-linear analyses of shear critical reinforced concrete frame using ETABS, Seismostruct.
ii. To understand the seismic behavior of shear critical reinforced concrete frame with respect to Global strength, Global stiffness, Ductility & Failure modes.
iii. To assess the accuracy of the FE software when predicting shear critical behavior using experimental data from another research.
iv. To propose a procedure for practitioners on how to improve the accuracy of popular commercial software when trying to predict shear critical behavior.

1.4 Significance of the study

i. This study contributes significant knowledge in understanding behavior of shear critical reinforced concrete frames under seismic actions, adding to the limited number of researches done so far on shear critical structures.

ii. The outcome of this research will also provide practicing engineers with a procedure to follow while performing performance analysis on shear critical structures.

1.5 Scope of the study

- Due to the limitations of laboratory test equipment a 2D non-linear finite element analysis is performed.
- Only static pushover analysis is carried out.
- All analyses are done assuming perfect bond between reinforcement and concrete, neglecting bond slip.

1.6 Methodology

Due to the lack of laboratory test equipment, a 2D non-linear analysis of a shear critical reinforced concrete frames is carried out using three finite element programs ETABS, Seismostruct and Vector 2. All data including reinforcement, and concrete material definitions; cross-sectional dimension and size of the members; laterally applied load; test setup and boundary conditions are taken from previously done experimental program by Kien Vinh Duong, Shamim A. Sheikh, and Frank J. Vecchio. [1]

Preferable models for reinforcement and concrete are selected and used in the finite element program based on their respective manuals and recommendation from appropriate literature. A perfect bond is assumed while modelling the frame since adequate anchorage was provided in the test frame.

Once analyses are done on the FE software all results are validated and further evaluated with respect to their accuracy in predicting behaviors of the shear critical frame such as, Global strength, Global stiffness, Ductility, Failure modes and Crack widths.

Finaly a procedure to improve the accuracy of the analysis steps commonly followed in the software, ETABS when predicting shear behavior will be set out. This will involve the use of specialized supporting software, Response 2000.

1.7 Organization of the study

This thesis is composed of five chapters. Chapter 1 presents the background, statement of the problem, objectives, significance of the study, and scope of the study. Chapter 2 provides a literature review of the existing literature in the relevant field of the research in this thesis. It covers theoretical background on Performance assessment of shear critical frames, Pushover analysis, non-linearity models and it covers state of the art review on tests conducted on shear critical frames. Chapter 3 provides the methodology used in this study. It discusses the experimental specimens for model validation, cross-sectional dimension and size of the members; laterally applied load; test setup and boundary conditions for the current analytical study and it also provides the material property, test setup, and restraint condition of the test frame. Finite element modelling using ETABS, Seismostruct and Vector 2. Chapter 4 presents the analytical result in comparison to the experimental data in order to validate the nonlinear finite element models. This will be followed by discussion and comparison of the results. The final chapter, Chapter 5, presents the conclusions drawn from the findings of this study as well as recommendations for future work.

CHAPTER 2 LITERATURE REVIEW

2.1 Introduction

During the last decades, structural engineers have made first rate advances in expertise the seismic performance of structures. This knowledge, mixed with improved modern-day-day practice, enables us to now not only layout structures that could competently withstand excessive earthquake loads without fatal collapse, but additionally to design buildings that may remain absolutely operational after an earthquake. However, we have no such certainty concerning the overall performance of buildings built in the past.

A few structures from that time have failed, or will fail, in a brittle manner in the course of a significant earthquake, especially due to the fact the principles of ductility and energy dissipation were not implemented in older codes. The latest Codes on the other hand set forth seismic design and detailing rules. [3]

If buildings that were constructed several many years in the past have been assessed in keeping with today's codes, many of them might be considered non code compliant. Further, some recently constructed structures can also be considered non code compliant if there is a construction error involved. These types of structures still exist and are still in use, creating the need to assess and improve the performance of these structures.

Although the dominant mode of failure in reinforced concrete frame structures is via flexure shear critical structures also exist and require close attention.[1]

The need to assess performance of existing structures is fast growing in Ethiopia since revised Ethiopian building code (ES EN1998:2015) shows a major change on the expected peak ground acceleration for major cities including the capital, Addis Ababa The reclassification on hazard map has caused the peak ground acceleration to be doubled from 0.05g to 0.1g. Furthermore, the ductility class has been upgraded from DCL to DCM. While the structures designed to the current requirements are expected to have ductile behavior structures designed to previous codes cannot be expected to do the same.[20]

In practice, reinforced concrete structures are typically designed based on linear elastic principles. Analysis procedures that follow these principles are generally plausible if the buildings are designed according to code. In other words, strength and serviceability requirements are met, joints are detailed correctly, rebar lengths are developed sufficiently, and failure modes are ductile. Buildings designed to the latest codes are detailed to ensure ductile behavior. The precise knowledge of their structural behavior is not necessary, but rather these buildings are designed to withstand the load requirements safely while ensuring ductile behavior.

Whenever existing buildings are inspected and deemed to be deficient according to current standards, a more accurate structural analysis is required to reassess the capacity of these deficient buildings for safety. For these buildings, second-order effects such as material and geometric nonlinearities become prominent. These effects can influence the ultimate capacity and failure mode; therefore, a detailed structural analysis is required to account for these second-order effects. Such an analysis will not only be useful for evaluating the rehabilitation strategy, but also provide a predicted cracking pattern that can be used as a forensic tool to warn engineers of potential failure. The nonlinear response of reinforced concrete structures has to be developed to a sufficient level of confidence in order to assess the seismic behavior of deficient buildings, and to implement repair strategies where needed.[1]

Most currently available analysis tools can easily model flexural failure mechanism by the use of moment hinges. However, most analysis software do not consider shear effects by default. These commonly used FE tools are practically used by most practitioners and may give inaccurate and unsafe predictions of strength and ductility for shear critical structures. The other reason to doubt this assumption of ductility during performance analysis is unlike current codes the older codes didn’t enforce stringent seismic design guide lines and detailing rules that ensure ductile behavior.

Two common deficiencies in inadequate buildings relate to moment and shear. Reinforced concrete structures that are inadequate in moment have been well studied, and there exist numerous reliable analytical tools that can be used to evaluate the structural reliability of such buildings. On the other hand, reinforced concrete framed structures that are deficient in shear have not been well studied, and reliable analytical tools to accurately evaluate shear-critical buildings are scarce. This lag in shear research is directly correlated to the complex nature of predicting shear behavior. Engineers have only recently developed the theoretical models to fully understand shear behavior through principles such as the

Compression Field (Collins 1978) and Modified Compression Field theories (Vecchio and Collins 1986).[16]

Although we may not know when existing shear-critical buildings might fail, we do know how they will fail. Unlike building failing in flexure which possess more ductility, shear-critical failures are extremely dangerous due to their brittle nature. The potential danger of such failures is all too clearly demonstrated by many lives lost in the 1995 Kobe earthquake: a tragedy caused by the catastrophic shear failure of numerous buildings.[27]

2.2 Pushover Analysis

Assessing the performance of existing structures commonly involves using a static nonlinear pushover analysis, which estimates the strength and deformation demands of a structural system in design earthquakes. This analysis compares the estimated demands to available capacities at specified performance levels. The assessment considers important parameters such as global and inter story drift, inelastic member deformations, & frame and connection forces. [13]

The pushover analysis is anticipated to offer insight into various response characteristics that cannot be obtained through elastic static or dynamic analysis. These response characteristics encompass:

- Realistic force requirements for potentially fragile elements, such as axial force requirements for columns, force requirements for brace connections, moment requirements for beam-to-column connections, shear force requirements in deep reinforced concrete spandrel beams, and shear force requirements in unreinforced masonry wall piers, among others.
- Estimates of deformation requirements for elements that need to deform inelastically to dissipate the imparted energy.
- Implications of individual element strength deterioration on the structural system's behavior.
- Effects of individual element strength deterioration on the structural system's behavior.
- Identification of critical regions with expected high deformation requirements, requiring focused detailing.
- Identification of strength disparities in plan elevation leading to changes in elastic range dynamic characteristics.

- Estimates of inter-story drifts considering strength or stiffness disparities, useful for damage control and P-Delta effect evaluation.

- Validation of the completeness and sufficiency of load paths, encompassing all structural system elements, connections, significant strength nonstructural elements, and the foundation system. [9]

Pushover analysis also known as a non-linear static analysis is also is a non-linear analysis procedure to predict the strength capacity of a structure past its yield point (meaning Limit State) up to its ultimate strength in the nonlinear post yielding range. In the process, the method also predicts potential failure points in the structure, by keeping track of the propagation of yielding (i.e. hinge formation) of each and every member in the structure (by use of 'hinges').

Hinges are points on a structure where one expects cracking and yielding to occur in relatively higher intensity so that they show high flexural (or shear) displacement, as it approaches its ultimate strength under cyclic loading. These are locations where one expects to see cross diagonal cracks in an actual building structure after a seismic mayhem, and they are found to be at the either ends of beams and columns, the 'cross' of the cracks being at a small distance from the joint – that is where one is expected to insert the hinges in the beams and columns of the corresponding computer analysis model. Hinges are of various types – namely, flexural hinges, shear hinges and axial hinges. The first two are inserted into the ends of beams and columns. Since the presence of masonry infills have significant influence on the seismic behavior of the structure, modelling them using equivalent diagonal struts is common in pushover analysis, unlike in the conventional analysis, where its inclusion is a rarity.

Basically, a hinge represents localized force-displacement relation of a member through its elastic and inelastic phases under seismic loads. For example, a flexural hinge represents the moment-rotation relation of a beam of which a typical one is as represented in Figure 2-1. AB represents the linear elastic range from unloaded state A to its effective yield B, followed by an inelastic but linear response of reduced (ductile) stiffness from B to C. CD shows a sudden reduction in load resistance, followed by a reduced resistance from D to E, and finally a total loss of resistance from E to F. Hinges are inserted in the structural members of a framed structure typically. These hinges have non-linear states defined as 'Immediate Occupancy' (IO), 'Life Safety' (LS) and 'Collapse Prevention' (CP) within its ductile range. This is usually done by dividing B-C into four parts and denoting IO, LS and CP, which are states of each individual hinges (in spite of the fact that the structure as a whole too have these states defined by drift limits). There are different criteria for dividing the segment BC. For instance, one such specification is at 10%, 60%, and 90% of the segment BC for IO, LS and CP respectively.[19]

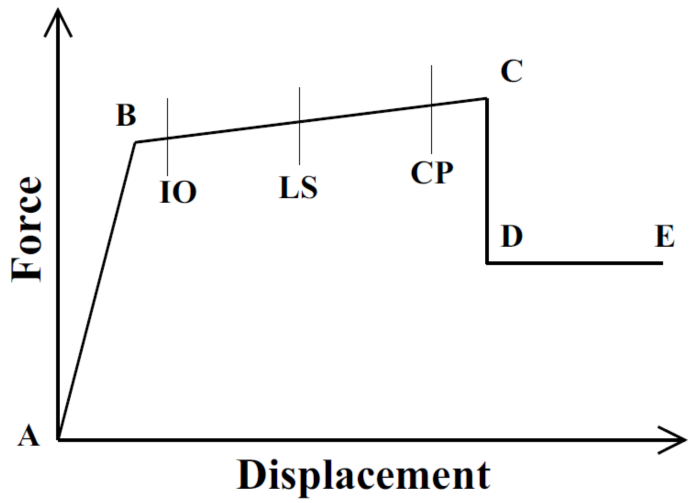

Figure 2-1: ***A-B-C-D-E curve for Force vs. Displacement***

2.2.1 Static Pushover vs Static Adaptive Pushover

2.2.1.1 Static Pushover

In pushover analysis both the force distribution and the target displacement are based on the assumptions that the response is controlled by the fundamental mode and that the mode shape remains unchanged after the structure yields. Therefore, the invariant force distributions do not account for the change of load patterns caused by the plastic hinge formation and changes in the stiffness of different structural elements. That could have some effects in the outcome of the method depending on different structural parameters.

In Static Pushover the applied incremental load P is kept proportional to the pattern of nominal loads (P°) initially defined by the user: $P = \lambda(P°)$. The load factor λ is automatically increased by the program until a user-defined limit, or numerical failure, is reached.

For the incrementation of the loading factor, different strategies may be employed, two types of control are commonly used: load and response control.

- Load Control; Refers to the case where the load factor is directly incremented and the global structural displacements are determined at each load factor level.
- Response Control; Refers to direct incrementation of the global displacement of one node and the calculation of the loading factor that corresponds to this displacement.

Conventional pushover analysis features an inherent inability to account for the effects that progressive stiffness degradation, typical in structures subjected to strong earthquake loading, has on the dynamic response characteristics of structures, and thus on the patterns of the equivalent static loads applied during a pushover analysis. Indeed, the fixed nature of the load distribution applied to the structure ignores the potential redistribution of forces during an actual dynamic response, which pushover tries to somehow reproduce. Consequently, the resulting changes in the modal characteristics of the structure (typically period elongation) and consequent variation in dynamic response amplification are not accounted for, which might introduce non-negligible inaccuracies, particularly in those cases where the influence higher mode is, or becomes, significant. These effects can only be accounted for by means of Adaptive Pushover.

2.2.1.2 Static Adaptive Pushover

Adaptive pushover analysis is employed in the estimation of the horizontal capacity of a structure, taking full account of the effect that the deformation of the latter and the frequency content of input motion have on its dynamic response characteristics. It may be applied in the assessment of both buildings as well as bridge structures.

In the adaptive pushover approach, the lateral load distribution is not kept constant but rather continuously updated during the analysis, according to the modal shapes and participation factors derived by eigenvalue analysis carried out at each analysis step. This method is fully multi-modal and accounts for the softening of the structure, its period elongation, and the modification of the inertia forces due to spectral amplification (through the introduction of a site-specific spectrum).

An adaptive pushover analysis method improves the accuracy of the analysis in predicting the seismic-induced dynamic demands of the structures. Conventional (non-adaptive) pushover analysis is frequently utilized to estimate the horizontal capacity of structures featuring a dynamic response that is not significantly affected by the levels of deformation incurred (i.e. the horizontal load pattern, which aims at simulating dynamic response, can be assumed as constant).

Apart from force distributions, adaptive pushover is also able to efficiently employ deformation profiles. Due to its ability to update the lateral load patterns according to the constantly changing modal properties of the system, it overcomes the intrinsic weaknesses of fixed-pattern displacement pushover and provides a more accurate performance-oriented tool for structural assessment, providing better response estimates than existing conventional methods, especially in cases where strength or stiffness irregularities exist in the structure and/or higher mode effects might play an important role in its dynamic response.

The adaptive algorithms, implemented in most analysis software, are very flexible and can accept a number of different parameters that suit the specific requirements of each particular project. For example, both SRSS and CQC modal combination methods are supported and the number of modes considered is explicitly defined, whereas users can also choose to update only the increment of loads applied at each step or the total loads already applied throughout the process up to the current point.

2.2.2 Performance Assessment criterion

Results of a performance analysis may be used to determine structural performance level of a given structure. FEMA 356 categorizes structural performance level of a building in to four discrete Structural Performance Levels and two intermediate Structural Performance Ranges. The discrete Structural Performance Levels are Immediate Occupancy (S-1), Life Safety (S-3), Collapse Prevention (S-5), and Not Considered (S-6). The intermediate Structural Performance Ranges are the Damage Control Range (S-2) and the Limited Safety Range (S-4). [10]

Immediate Occupancy Performance Level (S-1): Immediate Occupancy is the post-earthquake damage state in which only very limited structural damage has occurred. In the primary concrete frames, there will be hairline cracking.

Damage Control Performance Range (S-2): Structural Performance Range S-2, Damage Control, is the continuous range of damage states that less damage than that defined for the Life Safety level, but more than that defined for the Immediate Occupancy level.

Life Safety Performance Level (S-3): Structural Performance Level S-3, Life Safety, is the post-earthquake damage state in which significant damage to the structure has occurred, but some margin against either partial or total structural collapse remains. In the primary concrete frames, there will be extensive damage in the beams. There will be spilling of concrete cover and shear cracking in the ductile columns

Limited Safety Performance Range (S-4): Structural Performance Range S-4, Limited Safety is the continuous range of damage states between the Life Safety and Collapse Prevention levels

Collapse Prevention Performance Level (S-5): Structural Performance Level S-5, Collapse Prevention, is the building is on the verge of experiencing partial or total collapse. In the primary concrete frames, there will be extensive cracking and formation of hinges in the ductile elements

Table 2-1 further elaborates the structural performance levels for various elements of reinforced concrete structures.[10]

Table 2-1: Structural performance levels and damages

Elements	Type	Structural Performance Levels: Collapse Prevention S-5	Life Safety S-3	Immediate Occupancy S-1
Concrete Frames	Primary	Extensive cracking and hinge formation in ductile elements. Limited cracking and/or splice failure in some nonductile columns. Severe damage in short columns.	Extensive damage to beams. Spalling of cover and shear cracking (<1/8" width) for ductile columns. Minor spalling in nonductile columns. Joint cracks <1/8" wide.	Minor hairline cracking. Limited yielding possible at a few locations. No crushing (strains below 0.003).
	Secondary	Extensive spalling in columns (limited shortening) and beams Severe joint damage. Some reinforcing buckled.	Extensive cracking and hinge formation in ductile elements. Limited cracking and/or splice failure in some nonductile columns. Severe damage in short columns.	Minor spalling in a few places in ductile columns and beams. Flexural cracking in beams and columns. Shear cracking in joints <1/16"
	Drift	4% transient or permanent	2% transient; 1% permanent	1% transient; negligible permanent
Concrete Diaphragms		Extensive crushing and observable offset across many cracks.	Extensive cracking (<1/4" width). Local crushing and spalling.	Distributed hairline cracking. Some minor cracks of larger size (<1/8" width).

2.3 Non-Linearity Models

Accurate information about seismic behavior come at a cost of additional analysis effort required to incorporate all important elements together with their inelastic load deformation characteristics. The seismic behavior of a moment frame is highly affected by second order effects such as material nonlinearities, geometric nonlinearities, concrete shrinkage, tension stiffening effects, shear deformations and membrane action. This study will focus primarily on the influence of shear effects on the global behavior of a frame structure.

Reinforced concrete structures would not elastically respond to the maximum earthquake expected during the life of the structures. The determination of the behavior of structural components is essential for the assessment of the inelastic response of the complete structure. The initial stiffness, ultimate capacity and ductility demand are some of the parameters needed for this purpose. Due to complex interactions between various components of real structures, it is not possible to determine the dynamic characteristics only from dynamic tests of scale models. Furthermore, the cost of such tests is often substantial especially for large-scale specimens.

These difficulties have largely been overcome by static tests on structural components (e.g., beams, columns and shear walls) and small-scale structural subassemblies (e.g., beam-column joints) under cyclic load reversals. Results from these tests have been used to develop and calibrate analytical models. These analytical models have then been used to evaluate the nonlinear response of complete structures consisting of similar components for which the models were developed. Since the computational cost for data processing and storage was prohibitive, such analytical assessments could only be done for simple models. However rapid advancements in computing power in the past three decades has permitted the use of more complex nonlinear models, thereby reducing dependence on tests of scale models and simple analytical models.[6]

Appropriate choice of non-linearity model is of vital importance for accurate analysis of structures. Several models have been proposed to date for the simulation of the nonlinear behavior of reinforced concrete frame structures. These range from simple nonlinear springs which lump the behavior of an entire story into a one degree-of-freedom system to complex three-dimensional finite element formulations that describe the structural behavior by integrating the stress-strain relationships of the constituent materials (Filippou and Issa, 1988). [13]

These nonlinear models can be categorized, in a broader sense, into three categories:

(1) Global Models: These models constitute the simplest form of all nonlinear models, requiring the least computational power. In these models, the nonlinear behavior of the entire structure is concentrated at selected degrees of freedom. These models are useful for preliminary analyses and for rough estimates of the inter-story drifts and ductility demands. An accurate representation of the structural response should not be expected through the use these models.

(2) Discrete Finite Member Models: These models possess more advanced formulations compared to global models, and require more computational power. In these models, the structure is represented by an assemblage of interconnected elements that describe the

nonlinear behavior of reinforced concrete members. The nonlinearity in the constituent materials is introduced either at the element level in an average sense or at the section level as a more advanced case. Consequently, two types of element formulations are possible with the discrete finite member models: lumped nonlinearity member model, and distributed nonlinearity member model. [13]

The nonlinear behavior of reinforced concrete frames tends to be concentrated at the ends of beams or columns in the case of seismic loading conditions and at the midspans in the case of static loading conditions. Therefore, an early means of modelling this behavior was through the use of zero length plastic hinges as nonlinear springs located at the critical locations and connected by linear-elastic elements. Depending on the formulation, these models may incorporate a number of springs connected in series or in parallel.

Clough and Johnston (1966) introduced the earliest parallel component model allowing for a bilinear moment-rotation (M-φ) relation. As depicted in Figure 2-2(a), this element consists of two parallel elements: one elastic-perfectly plastic to simulate yielding and the other perfectly elastic to represent strain-hardening. Takizava (1976) generalized this model to multilinear monotonic behavior to take account of the cracking of the concrete. Giberson (1967) formally introduced the series model although it had been reportedly used earlier. As shown in Figure 2-2(b), this model consists of a linear-elastic element with one equivalent nonlinear rotational spring attached to each end in which the inelastic deformations of the member are lumped. This model is more versatile than the original Clough model because more complex hysteretic behavior can be described.

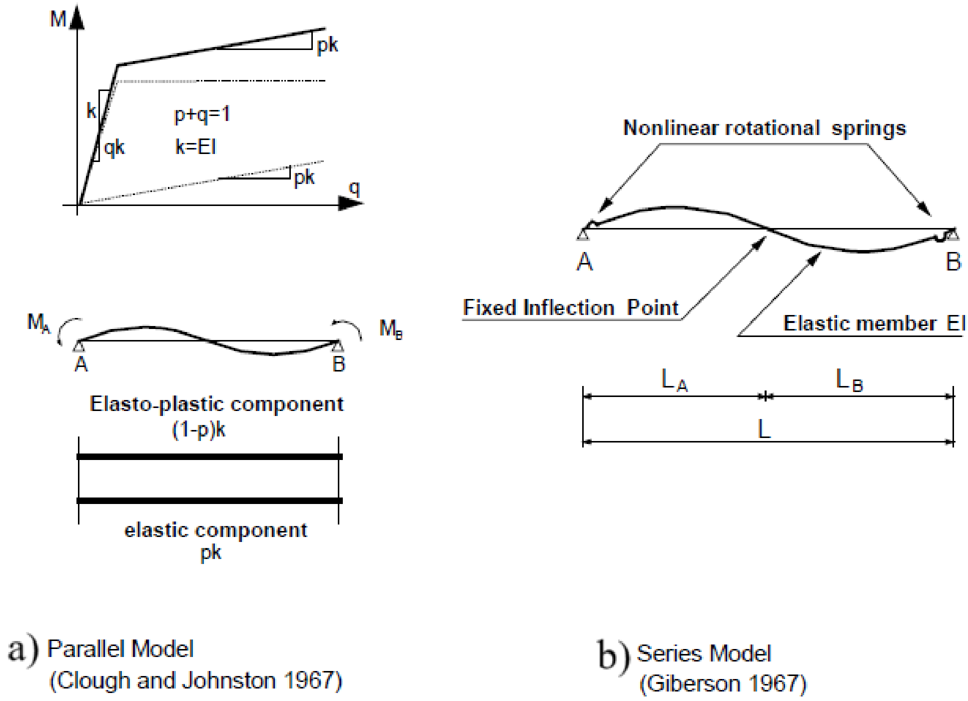

Figure 2-2: Lumped Plasticity Elements: (a) Parallel Model (Clough and Johnston, 1966); (b) Series Model (Giberson, 1967)

(3) Microscopic Finite Element Models: These models possess the most advanced formulations developed to date for nonlinear analyses, requiring significant computational power and analysis time. In these models, members and joints are discretized into a large number of finite elements. Constitutive and geometric nonlinearity are typically accounted for at the stress-strain level or averaged over a finite region. Bond modelling between concrete and reinforcement, interface friction at the cracks, creep, relaxation, thermal effects and geometric crack discontinuities are among the physical nonlinearities usually considered by this class of models.

2.3.1 Distributed Nonlinearity Models

In distributed nonlinearity models, material nonlinearity can take place at any element section. The element behavior is formulated from weighted integration of the sectional responses. Element integrals are evaluated numerically; therefore, only the behavior of selected sections along the integration points is monitored. The primary unknowns of the model are either the element deformations or the element forces, which are determined through proper interpolation functions from the global element displacements or forces, respectively. Discrete cracks are treated as smeared over a finite length. The constitutive behavior of the cross section is either formulated according to classical plasticity theory or is explicitly derived by discretization of the cross section into fibers, as in the case of the spread plasticity models.

Nonlinearity model elements can be formulated in the context of either displacement-based or force-based approaches. Displacement-based approach uses classical finite element formulations to derive the element stiffness matrix and the element restoring force vector. This approach is used widely as it can be conveniently implemented into a general-purpose finite element framework. However, in the case of reinforced concrete frames where material nonlinearities are considered, the displacement-based approach is approximate, requiring refined meshes for satisfactory simulation of the frame response.

Force-based formulations, on the other hand, provide exact solutions regardless of the variations in the beam cross section and material nonlinearity. Computing element resisting forces, however, is a much more complex issue in force-based formulations, arising from the impossibility of directly relating section resisting forces and element resisting forces, as in the case of the displacement-based approach. An iterative method proposed by Spacone et al. (1996) can be used for this purpose. Although there are more computations involved in a force-based approach than in the displacement-based approach, the precision of the force-based approach permits the use of a single element per structural member, thereby giving way to significant reductions in the global degrees of freedom of the structure. [26]

2.3.2 Fibre Models

Fibre models constitute the most advanced formulation in distributed nonlinearity models. In these models, the element is subdivided into longitudinal fibres as shown in Figure 2-3. The fibre location in the local y, z reference system and the fibre area A are fibre geometric characteristics of the cross section. The governing compatibility relationship is based on the “plane sections remain plane” hypothesis, which forms the basis of the engineering beam theory used in the sectional analysis of concrete members. Equilibrium is satisfied through integrating the responses of the fibres and equating them to the required sectional forces.[8]

Appropriate stress-strain relationships are used for the constituent materials so as to determine the stress distribution on the section for a given strain profile. The first force-based fibre element model, proposed by Kaba and Mahin (1984), takes into account only uniaxial bending. In this model, the sectional deformations are computed from the element deformations through the use of flexibility-dependent deformation shape functions. Fibre strains are then calculated using sectional deformations, through which fibre stresses and stiffnesses are determined. The section stiffness matrix is assembled and inverted to obtain the flexibility matrix. Although yielding promising results, this model is reported to have convergence problems (Taucer,1991) and is unable to consider element softening. Zeris and Mahin (1988 and 1991) extended the formulation of Kaba and Mahin (1984) to the biaxial bending case. [8]

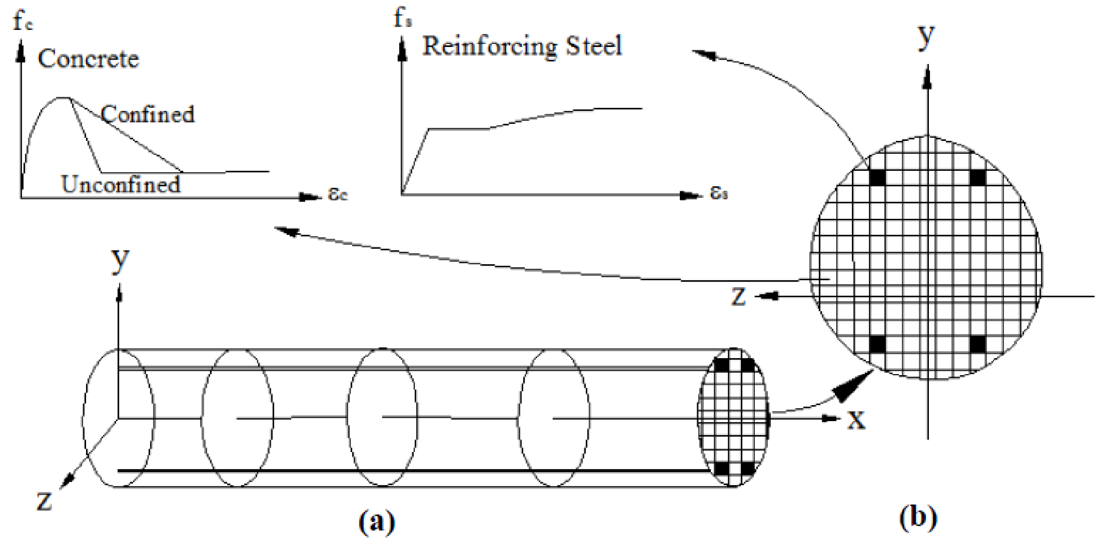

Figure 2-3 Fibre Element: (a) Distribution of Control Sections; (b) Section Subdivision into Fibres (Taucer et al, 1991)

Distributed inelasticity elements are becoming widely employed in earthquake engineering applications, either for research or professional engineering purposes. This can be implemented with two different finite elements (FE) formulations: the classical displacement-based (DB) ones [e.g. Hellesland and Scordelis 1981; Mari and Scordelis 1984], and the more recent force-based (FB) formulations [e.g. Spacone et al. 1996; Neuenhofer and Filippou 1997].

In a DB approach the displacement field is imposed, whilst in a FB element equilibrium is strictly satisfied and no restraints are placed to the development of inelastic deformations throughout the member; see e.g. Alemdar and White [2005] and Freitas et al. [1999] for further discussion. In the DB case, displacement shape functions are used, corresponding for instance to a linear variation of curvature along the element.

2.4 Tests on Shear critical Fames

At the University of Toronto, Kien Vinh Duong, Shamim A. Sheikh, and Frank J. Vecchio constructed and tested a two-story reinforced concrete frame with shear-critical beams. The frame underwent lateral reverse cyclic testing until severe shear damage occurred, after which it was repaired using carbon fibre reinforced polymer (CFRP) and retested.

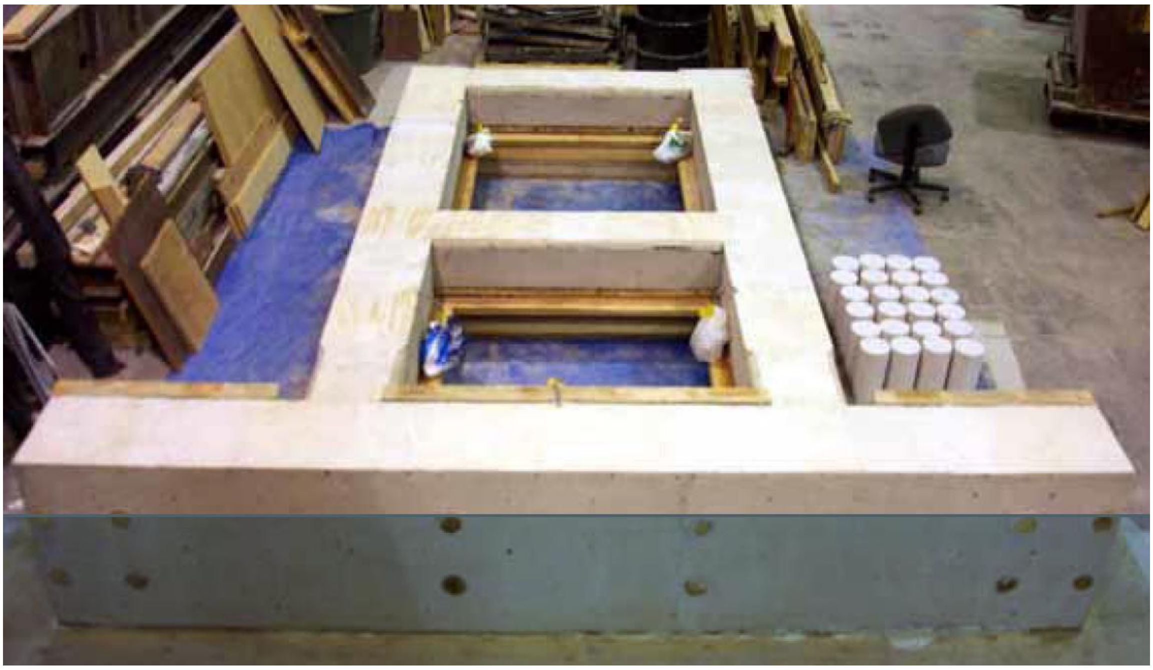

Figure 2-4 Duong Frame after Construction and Casting

During Phase A, the frame underwent lateral reverse cyclic testing until the beams experienced extreme shear damage. Following this, Phase B involved repairing the beams using carbon fiber-reinforced polymer (CFRP) and retesting the frame.

The clear covers for the beams, columns, and base were 30 mm, 20 mm, and 40 mm, respectively. The testing setup included a vertical and lateral loading system, as well as an out-of-plane bracing system. Vertical column loads were applied using four hydraulic jacks, with a constant load of 420 kN per column. Utilizing a displacement-controlled actuator at the top storey beam centreline, horizontal loading was applied.

During forward half-cycle phase A, load stages were recorded at increment of 25 kN or at significant changes in structural behavior. (i.e. cracking or sudden increase of crack width) In the reverse half-cycle of Phase A, the load increment was increased to 30 kN, and with only major cracks measured.

On Phase A the frame was loaded in the forward direction until shear failure was evident, then after unloading, the load was again applied in the opposite direction to a similar displacement magnitude reached in the forward phase.

In Phase B, the repaired beam was loaded in 12 cycles , this phase of testing took one week to complete, and the load cycles were performed in predetermined sequence based on the yield displacement of phase A.

In phase Δy, yield displacement of the frame was founde to be 25 mm, occurring at a global drift of 0.625%.

In the initial load stages some drop in load capacity was observed due to creep. Similarly large shear cracks resulted in a reduced load carrying capacity in the final set of load stages.

Test observations—Phase A

- In Phase A, the peak load capacity was estimated as close to 327 kN with a corresponding frame peak displacement of 44.7 mm.
- The failure mode is considered to be flexural- shear. This is evident since the beams incurred flexural cracks at a horizontal load of 75 kN. Then the lower beam cracked in shear at a horizontal load of 148 kN.
- The longitudinal reinforcement bars yielded at a horizontal load of 295 kN in the the first-story beam. Transverse reinforcement yielding also occurred at a load of 320 kN.
- In the final stage the maximum shear crack width was 9 mm and 2 mm for first and second story beams respectively.
- Following its unloading, the frame still remained with a residual deformation of 11 mm from its peak displacement.
- Phase A, total collapse of the frame was not achieved. However the load capacity had reached its peak evident by the large shear cracks.
- Significant changes to the structural stiffness involved either notable shear cracking, or yielding of the longitudinal and transverse beam reinforcement.
- Initial lateral stiffness of 24 kN/mm was relatively constant until the first set of north column flexural cracks were developed at 99 kN

- Between 99 kN and 221 kN, the stiffness decreased to 12.6 kN/mm. shortly after the lower and upper beams exhibited shear cracks (at 125 kN and 197 kN, respectively). In addition, the south column developed flexural cracks at 125 kN.
- Between 221 kN and 320 kN, the stiffness decreased further to 6.1 kN/mm. By 320 kN, the upper and lower beam flexure and shear steel had yielded.
- From 320 kN to 327 kN, the stiffness was near zero at about 0.5 kN/mm.
- The unloading stiffness was -9.6 kN/mm.

It is important to point out that the peak lateral load of 327 kN was reached at 44.8 mm (average top story lateral displacement) during the last stage of the forward half-cycle. Collapse, as conventionally defined, did not take place. The first-story beam was heavily damaged in shear but the structural integrity of the frame was still intact.

Since repair of the beams was to take place, the loading was stopped to prevent any catastrophic beam failure. The peak load of the frame may have been slightly higher than 327 kN had the loading continued; however, judging by the 10+ mm shear crack width, the limit of the frame was nearly reached.

Towards the latter load stages of the forward half-cycle, all of the tensile longitudinal steel yielded (recall the yield strain for the No. 20 rebar was 2250 x10-6). During the forward half-cycle, five out of twelve stirrups yielded. These stirrups were located at regions of major shear cracks.

It was concluded that the damage mode during the forward half-cycle was combined flexural-shear, as evident by yielding of both the longitudinal and transverse steel. During the reverse half-cycle, the frame was damaged predominately in shear since only the transverse steel yielded.

Table 2-2 Summary of Net Horizontal Load and Lateral Drift

Phase A: Forward Half-cycle			
Load Stage	Net Horizontal Load (kN)	Avg. 2nd Story Lateral Displacement Δ_{st} (mm)	%Lateral Drift
1	25	0.76	0.02
2	51	1.60	0.04
3	75	2.65	0.07
4	99	4.13	0.10
5	125	5.46	0.14
6	148	7.41	0.19
7	174	9.60	0.24
8	197	11.70	0.29
9	221	13.80	0.35
10	246	18.00	0.46
11	272	21.70	0.54
12	295	25.50	0.64
13	320	30.00	0.75
14	325	32.30	0.81
15	327	44.70	1.12

CHAPTER 3 METHODOLOGY

3.1 General

In this study the seismic performance of a shear critical frame is investigated through finite element analysis using ETABS, Seismostruct and Vector 2. After the analyses validation will be done using experimental data from a laboratory test carried by Kien Vinh Duong, Shamim A. Sheikh, and Frank J. Vecchio at the University of Toronto.

In this chapter, the experimental specimens for model validation are described and their geometry and reinforcement details are presented. Following that, finite element modelling in ETABS, Seismostruct and Vector 2 which includes modelling of geometry, creating mesh, material properties, bond element, and restraint condition used to simulate the test are discussed. Finally, the validation of the nonlinear finite element models using the available experimental results is thoroughly discussed.

Finally, this paper uses experimental data from the aforementioned test to assess the accuracy of some commercial and educational finite element software and procedures in estimating the performance of a shear critical frame under lateral loads. Furthermore, a proposal will be made on a possible procedure to improve the accuracy of the modelling procedures in ETABS when predicting shear critical behavior.

3.2 Description of the Duong Frame

In this paper finite element analysis is carried out on a shear critical frame tested by Kien Vinh Duong at the University of Toronto. The frame was tested by applying constant vertical loads and incremental horizontal load until failure took place. Then a repair using carbon fibre reinforced polymer (CFRP) was done on the failed beams, then the test was repeated.

3.2.1 Frame Layout and Sectional Properties

The Doung frame is a single-span, two-story, shear-critical reinforced concrete frame with a fixed base condition was constructed and tested in the laboratories at the University of Toronto. The test frame had a height of 4.6 m and a width of 2.3 m.

Lateral reverse cyclic loading was applied at the top of this test specimen with the lateral force reacted off a strong wall that stood 4.62 m high. The height of the specimen was limited by the height of the strong wall, as well as the lab clearance. The beams had a width of 300 mm and a depth of 400 mm. The columns also beam had a width of 300 mm and a depth of 400 mm. The frame was supported of a reinforced concrete base of 800 mm width. The base was also of a thickness of 400 mm and a length of 4100 mm. The base was casted monolithically with the frame and post-tensioned to the floor. The beam had a clear span of 1500 mm.

The reinforcing steels used in the frame are No.10(11.3 mm), No.20(19.5 mm), and US No.3(9.5 mm). The beam sections had four No.20 bars shown in figure 3-3, with a transverse reinforcement of US No.3 at a spacing of 300mm. The columns had four No.20 bars shown in figure 3-3, with a transverse reinforcement of four legged No.10 at a spacing of 100mm. Refer to Figure 3-2 for the reinforcement layout, and Figure 3-3 for the as built member cross-sections.

The covers for beams and columns was 30 mm and 20 mm, respectively. For the base a cover of 40 mm cover was utilized.

The lateral loads applied to the frame at the top story induced high bending stresses at the base of the column and at the inner column faces at the top of the columns. In order to prevent premature column failure, an extra layer of longitudinal reinforcement consisting of four No.20 bars was added at each of these locations to increase their flexural capacity (refer Figure 3-2). Column splices were implemented at the second-story mid-height where stress levels were low under applied loading.

The horizontal load was provided by a 1000 kN capacity actuator mounted laterally against a reacting strong wall in a displacement-controlled mode.

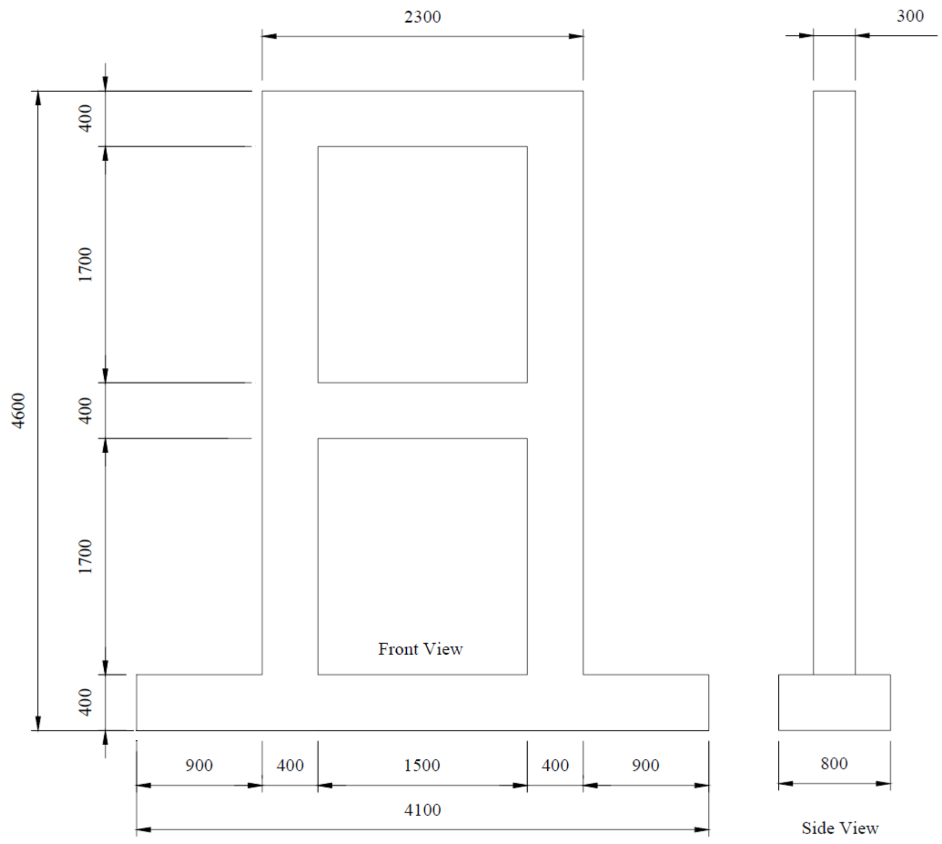

All dimensions are in mm.

Figure 3-1 Nominal Frame Dimensions

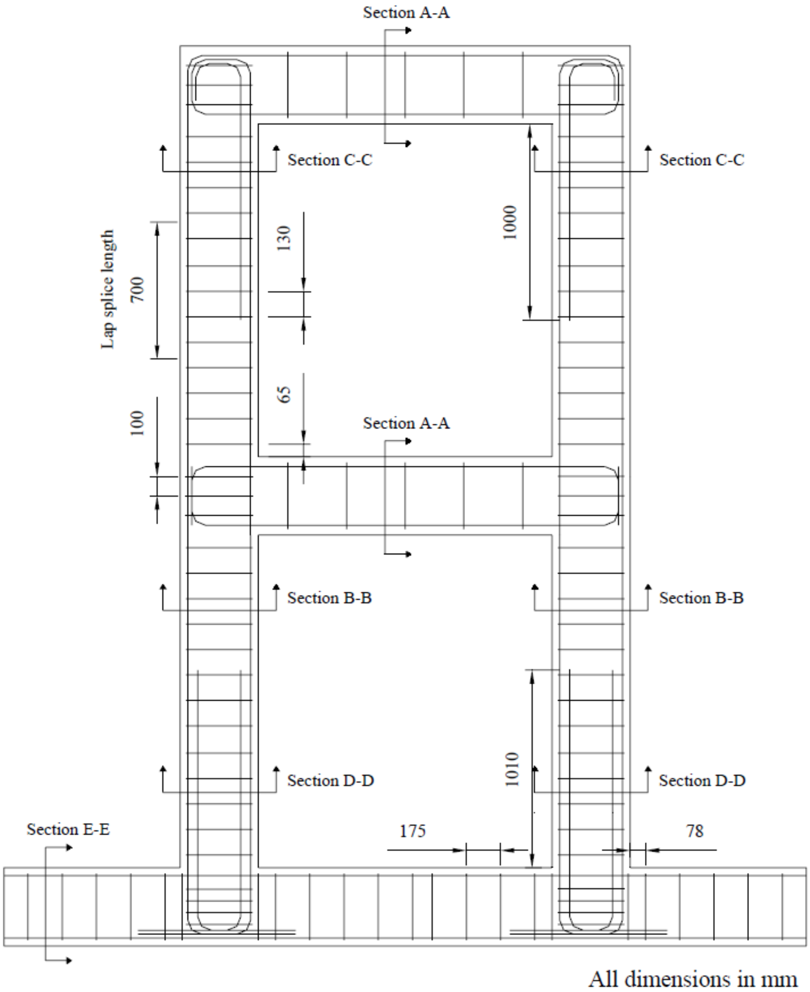

Figure 3-2 Frame Reinforcement Layout

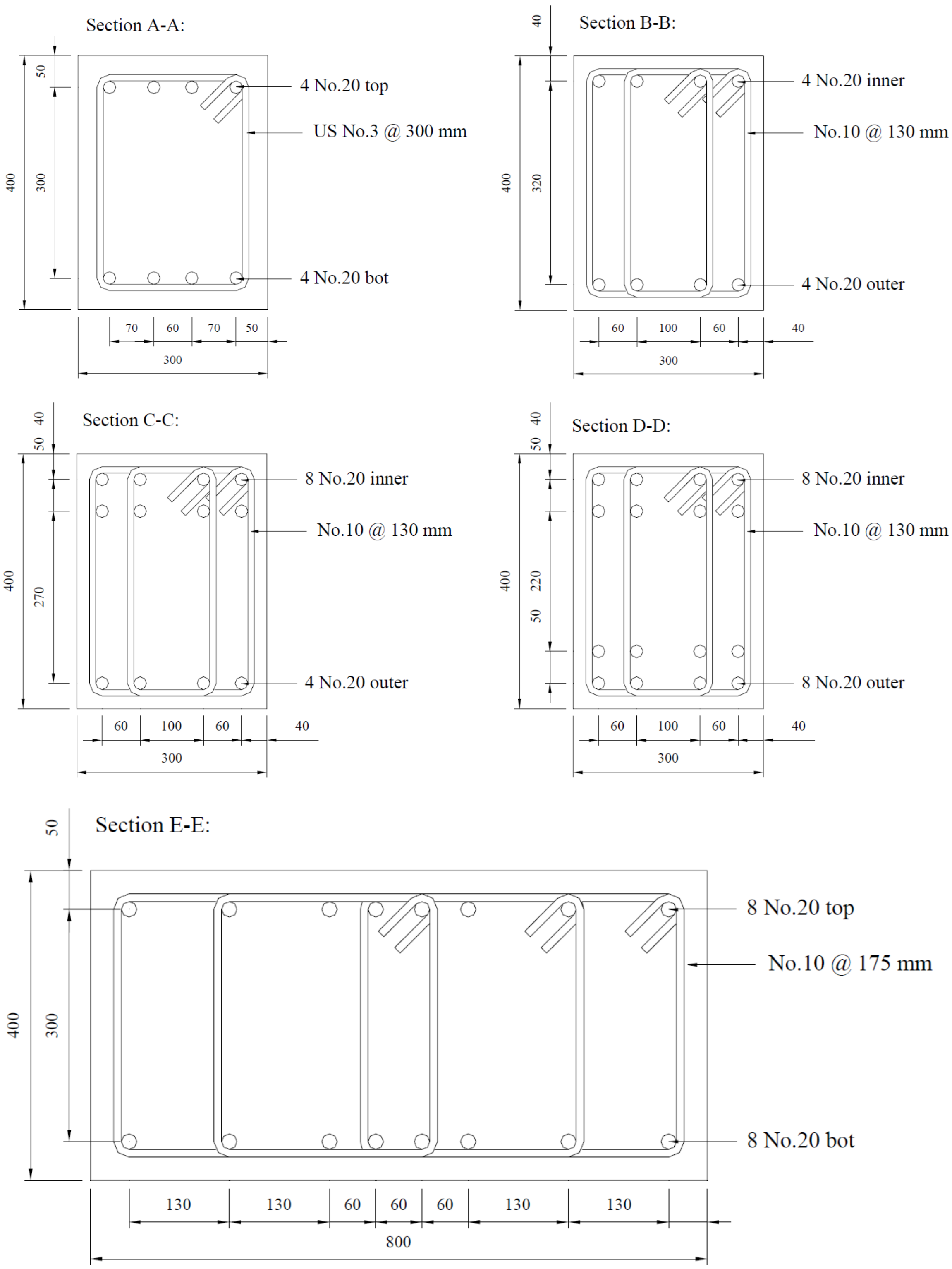

All dimensions are in mm.

Figure 3-3 Frame Member Cross Sections

3.2.2 Material Properties

Cylinder compression tests (150 mm in diameter and 300 mm in height) were performed according to the ASTM C39 Standard at 8 days, 28 days and on the day of testing. Cylinders were subjected to either lab or moist cured conditions, with the former subjected to the same curing condition as the specimen. The material properties of concrete and reinforcing steel are presented below

Table 3-1 Concrete Material Properties

Concrete Material Properties				
$f_c^{'}$ (MPa)	ε_0 ($x10^{-3}$)	E_c (MPa)	G_c (MPa)	μ
42.9	2.31	30058	13069	0.2

Three different sizes of deformed reinforcing bars were used in this experiment: No.10, No.20, and US No.3. Standard tensile tests were performed on a 1000 kN testing machine. Their nominal diameters, cross-sectional areas, and other relevant properties are presented in Table 3.2.

Table 3-2 Reinforcement Material Properties

	Reinforcement Material Properties							
	A_s (mm2)	d_b (mm)	f_y (MPa)	f_u (MPa)	E_s (MPa)	E_{sh} (MPa)	ε_{sh} ($x10^{-3}$)	ε_u ($x10^{-3}$
No. 20	300	19.5	447	603	198400	1372	17.1	130.8
No. 10	100	11.3	455	583	192400	1195	22.8	129.9
US #3	71	9.5	506	615	210000	1025	28.3	134.6

3.2.3 Test Setup

The testing setup composed of a vertical and lateral loading system, and a bracing system preventing out of plane movement. Vertical column loads were applied in the following manner through four hydraulic jacks. A constant vertical load of 420 kN was applied on each column while lateral loading was exerted via a displacement-controlled actuator placed at the mid depth of the second story beam.[1]

A reaction wall was used to support the actuator which had a 1000 kN capacity. Only pushing was applied to the frame regardless of the direction of the horizontal load to ensure consistency in forward and reverse cycles. While some axial compression is induced in the beams during load application these was not significant in magnitude to influence the shear behavior of the beams.

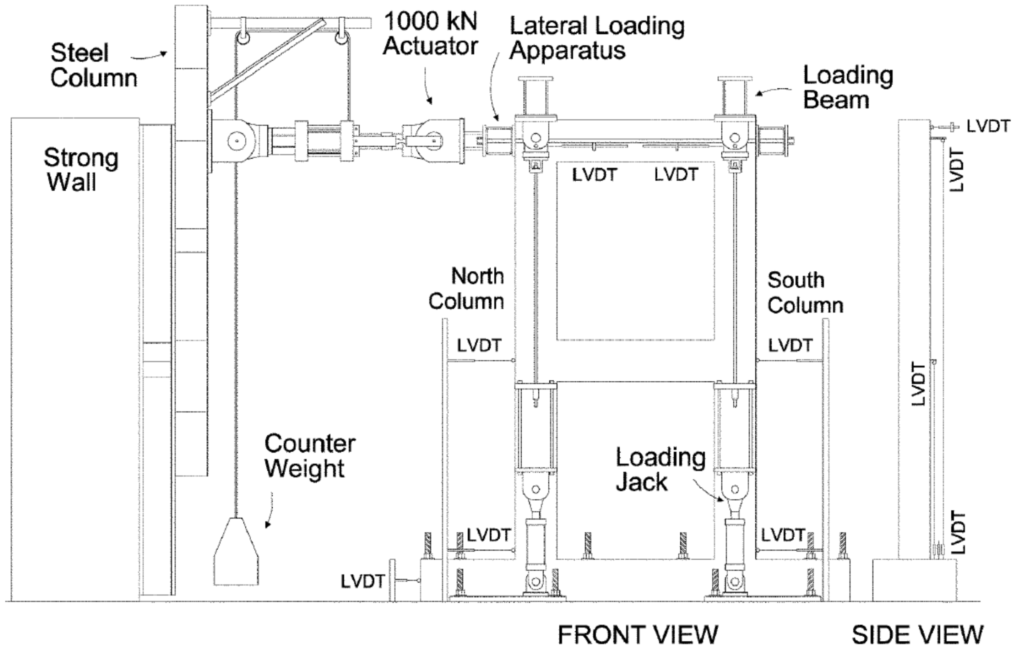

Figure 3-4 Duong Frame Test Setup

3.3 Modelling and Analysis with Vector 2

3.3.1 Introduction to Vector 2

VecTor2 is a nonlinear finite element program for the analysis of two-dimensional reinforced concrete membrane structures. The program has been developed at University of Toronto with experimental tests to corroborate the ability of VecTor2 to predict the load-deformation response of a variety of reinforced concrete structures exhibiting well-distributed cracking when subject to short-term static monotonic, cyclic and reverse cyclic loading. While VecTor5 was used in a study by Serhan Guner and Frank J. Vecchio for a pushover analysis of a shear critical frame, successfully, in this study we will use the two dimensional VecTor2 in attempt to replicate the results.

By combining a variety of realistic nonlinear models for reinforced concrete with the powerful analytical capabilities of finite element analysis, VecTor2 permits more accurate assessments of structural performance (strength, post-peak behavior, failure mode, deflections and cracking) than can be achieved by linear-elastic methods. At the same time, the finite element method allows analysts to address the composite nature of reinforced concrete material, changing material properties due to progressive cracking, challenging geometries and loadings – complexities which might thwart conventional analysis techniques.

The effective use of nonlinear finite element programs for the analysis reinforced concrete requires an understanding of the theoretical basis of programs and their operation. Therefore, rational and effective use of the programs requires guidance and user experience. VecTor2 comes with extensive user manual describing not only how to use the software but also the underlying principles for its formulation.

The theoretical bases of VecTor2 are the Modified Compression Field Theory (Vecchio and Collins, 1986) and the Disturbed Stress Field Model (Vecchio, 2000) – analytical models for predicting the response of reinforced concrete elements subject to in-plane normal and shear stresses. VecTor2 models cracked concrete as an orthotropic material with smeared, rotating cracks. The program utilizes an incremental total load, iterative secant stiffness algorithm to produce an efficient and robust nonlinear solution.

Finite element models constructed for VecTor2 use a fine mesh of simple elements with minimal nodes, straight conforming boundaries, and linear displacement functions. This methodology has advantages of computational efficiency and numerical stability. It is also well suited to reinforced concrete structures, which require a relatively fine mesh to model reinforcement detailing and local crack patterns. The element library includes a three-node constant strain triangle, a four-node plane stress rectangular element and a four-node quadrilateral element for modelling concrete with smeared reinforcement; a two-node truss-bar for modelling discrete reinforcement; and a two-node link and a four-node contact element for modelling bond-slip mechanisms.

3.3.2 Material modelling

In this study, a shear critical frame tested by Kien Vinh Duong at the University of Toronto, is modelled using the basic version of Vector2. In the following sections material models for concrete, reinforcing steels, and bond elements used in the finite element program are discussed in detail.

3.3.2.1 Concrete Elements

The VecTor2 element library is subdivided into three element categories depending on the type of material the element models. The first category consists of planar triangular, rectangular and quadrilateral elements which model concrete with or without smeared reinforcement. The second category consists of the linear truss bar element which models discrete reinforcement. The third category consists of the nondimensional link and contact elements, which model bond-slip.

Reinforced concrete elements are used to model plain concrete or concrete with smeared reinforcement, representing regions of a structure having well-distributed reinforcement. Owing to compatibility between the concrete and smeared reinforcement comprising the element, the concrete and reinforcement are perfectly bonded. The element stiffness matrices, [k], are formulated with the composite material stiffness matrices by closed form evaluation of the following integral:

$$[K] = \int_{vol} [B]^T [D][B] dv \tag{3.1}$$

Where,

$[B]$= element strain-displacement matrix

$[D]$= composite material stiffness matrix

In this study a plane stress rectangle, as shown in Figure 3-5, a four-nodded element with uniform thickness, t was used to model all concrete regions. The element is defined by four node numbers in counterclockwise sequence, i,,j,m,n. As each node translates in the x and y directions, the element has a total of eight degrees of freedom. The rectangle must be oriented so as its edges parallel to the x and y axes. Although the rectangle may assume any width and height, its accuracy degrades as the shape deviates from a square. As such, rectangles with aspect ratios exceeding 3:2 should be avoided.[maual]

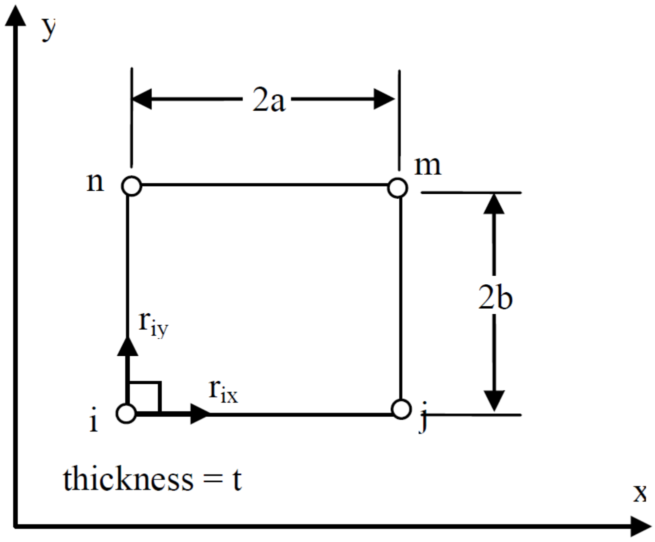

Figure 3-5 Plane stress rectangle element

3.3.2.2 Reinforcement Elements

Reinforcement elements are used to model reinforcement bars or FRP layers, or a lumped collection of them in close proximity relative to the surrounding element sizes. The stiffness matrix, [k], of these elements are formulated with the reinforcement material stiffness matrix only. Use of the discrete reinforcement elements is required when either the behavior of individual bars or bond-slip mechanisms are of interest. Generally, as a matter of accuracy and computational economy, primary reinforcement is modelled by discrete reinforcement elements whereas well-distributed reinforcement is modelled by smeared reinforcement in the reinforced concrete elements.

In this study a truss bar, was used to model all longitudinal reinforcement as shown in Figure 3-6, this is a two-nodded element with uniform cross-sectional area, A. The element is defined by two node numbers, i, j. As each node displaces in the x and y directions, the element has a total of four degrees of freedom. The truss element may assume any orientation in the x, y coordinate system. The truss bar exhibits resistance only to elongation along its axis.

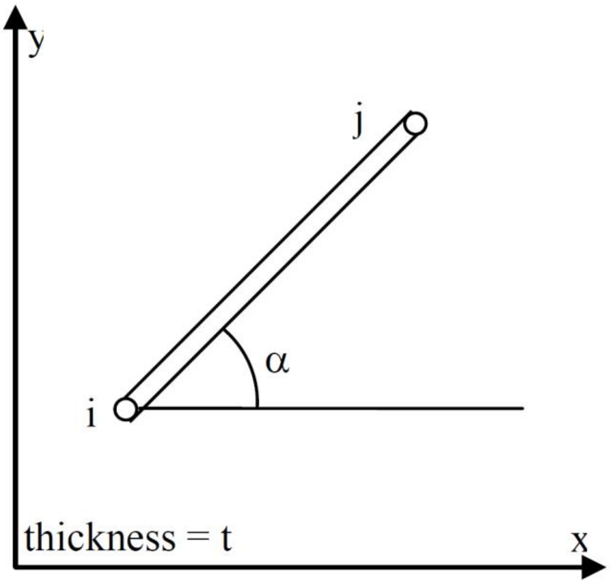

Figure 3-6 Truss bar element

3.3.2.3 Contact Elements

Vector2 by default uses a contact element, as shown in Figure 3-7, is a four-nodded element, having only a linear dimension. The element is defined by four different node numbers in the sequence, j, k, m, n. Prior to slippage, nodes, j and k must have the same coordinates. Either node j or node k must be attached to a reinforced concrete element. The other node must be attached to a discrete reinforcement element. The same condition applies to the nodes m and n. As each node displaces in the x and y directions, the element has a total of eight degrees of freedom. The contact element may assume any orientation in the x,y plane.

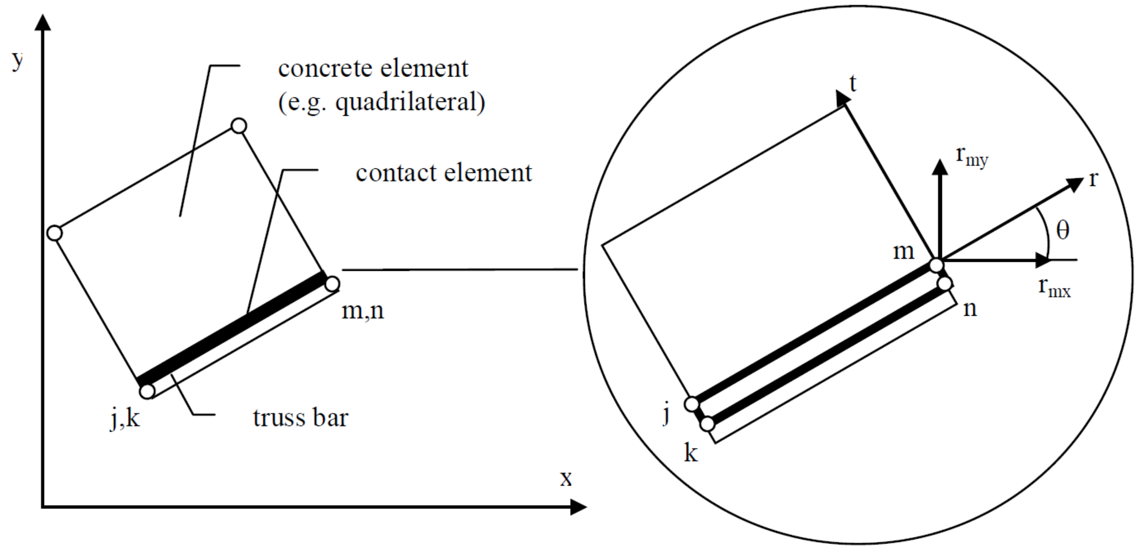

Figure 3-7 Contact element

3.3.2.4 Constitutive Models for Concrete Materials

The concrete constitutive and behavioral models are paramount to the accuracy of the VecTor2 results. At each load step, the structure stiffness is determined from the stresses and strains calculated from the constitutive models. Further, the inclusion or omission of a model determines whether the effects of pertinent behaviors are included in the analysis, and the suitability of the results to the purpose of the analysis. Many of the models in VecTor2 include multiple options differing in degree and type, which may produce a divergence of results.

Regarding the constitutive relationships, VecTor2 utilizes models, which describe the concrete response via nonlinear functions of stress and strain. This approach is amenable to concrete given that the combined behavior of aggregates, cement and reinforcement which that can often only be described by empirical relationships. These relationships typically involve mechanical properties determined from standard specimens under specific stress and strain conditions, rather than being inherent material properties. Bearing this in mind, it is necessary to select models judiciously for each analysis.

The following discussion describes the constitutive and behavioral models used in this study;

3.3.2.4.1 Compression Pre-Peak Response

The stress-strain response of concrete in uniaxial compression is nonlinear beyond low compressive stresses, despite the fact that the constituent cement paste and aggregates exhibit linear elastic behavior in compression. The apparent contradiction is explained by the softening effect of internal microcracks that form as a result of stress concentrations at the interface of the cement paste and aggregates. The ascending branch of the nonlinear stress-strain response is simulated using Compression Pre-Peak Response Models.

Compression pre-peak response models compute the principal compressive stress, fci, if the compressive principal strain, ε_{ci}, is less compressive than the strain, εp, corresponding to the peak compressive stress, f_p. The peak parameters are determined by adjusting the unconfined uniaxial concrete cylinder strength, f'_c, and the corresponding strain, εo, for compression softening due to transverse tensile strains, and strength enhancement due to confinement.

The default Compression Pre-Peak Response model on Vector 2 is the Hognestad parabola, a simple compression response curve, suitable for normal concrete strengths (<40 MPa). However, in this study the specific compressive strength of the concrete at the day of casting was 42.9MPa. Accordingly a Compression pre-peak response model of **Popovics (High Strength)** was utilized.

Experimental studies demonstrate that as the concrete strength increases, the response is linear to a greater percentage of the maximum compressive stress, the strain corresponding to the peak compressive stress increases, and the descending branch of the stress-strain curve declines more steeply. Also, intermediate high strength concretes exhibit a decreased ultimate compressive strain. The Popovics High Strength response curve, shown in Figure 3-8, exhibits a more rapid post-peak stress decay for higher strength concretes.

The stress-strain curve is given by the following equation:

$$f_{ci} = -\left(\frac{\varepsilon_{ci}}{\varepsilon_p}\right) f_p \frac{n}{n-1+\left(\varepsilon_{ci}/\varepsilon_p\right)^{nk}} \quad for\ \varepsilon_{ci} < 0 \tag{3.2}$$

Where,

f_{ci} = principal compressive stress

ε_{ci} = compressive principal strain

ε_p = concrete compressive strain corresponding to f_p

f_p = peak concrete compressive stress

The long fraction represents the deviation from linear-elastic response.

The curve fitting parameter, n, captures the greater linearity of higher strength concrete through the diminishing difference between the initial tangent stiffness E_c, and secant stiffness E_{sec}. It is given by the following equation:

$$n = 0.80 + \frac{f_p}{17} \quad \left(f_p \text{ in MPa} \right) \tag{3.3}$$

The parameter, k, increases the post-peak decay in stress and is calculated as follows:

$$k = \begin{cases} 1.0 & \text{for} \quad \varepsilon_p < \varepsilon_{ci} < 0 \\ 0.67 + \dfrac{f_p'}{62} \geq 1.0 & \text{for} \quad \varepsilon_{ci} < \varepsilon_p < 0 \left(f_p \text{ in MPa} \right) \end{cases} \tag{3.4}$$

Note that the Popovics – High Strength relationship predefines the initial tangent stiffness, Ec, as follows:

$$E_c = \frac{f_p}{|\varepsilon_p|} \cdot \frac{n}{n-1} \tag{3.5}$$

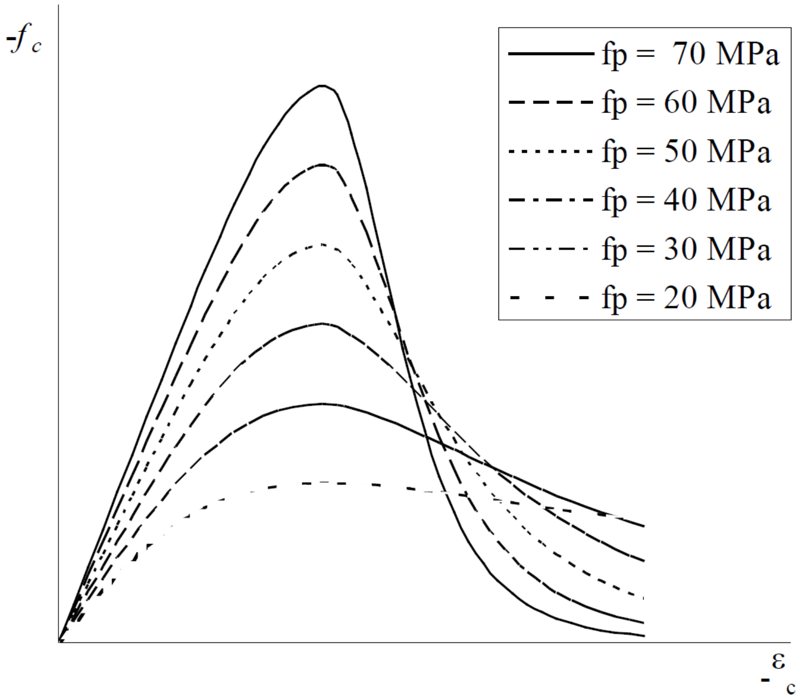

Figure 3-8 Popovics high strength pre- and post-peak concrete compression response

3.3.2.4.2 Compression Post-Peak Response

Beyond the peak compressive stress, f_p, and corresponding strain, ε_p, concrete resists substantial compressive stress under continued compressive straining. Moreover, confinement of the concrete by transverse stresses enhances the strength and ductility of the concrete, transforming the failure in compression from brittle to ductile. This residual compressive strength and ductility may allow localized regions of a reinforced concrete structure to fail, but gradually unload so as to redistribute internal stresses and forestall total failure of the structure until additional deformation occurs. The effect of such post-peak behavior may be beneficial by allowing greater economy in design, or detrimental, should overstrength of the desired failure mode result in an undesirable failure mode. Post-peak behavior may also be significant in over-reinforced structures. As such, the selection of the compression post-peak response is significant to a realistic analysis of the load-deformation response.

In this study the Modified Park-Kent compression post-peak response model is used to account for the enhancement of concrete strength and ductility due to confinement. On the stress-strain curve shown in Figure 3-9, The linearly descending branch of the modified stress-strain curve can be calculated as follows:

$$f_{ci}^{b} = -\left[f_p + Z_m f_p \left(\varepsilon_{ci} - \varepsilon_p \right) \right] < 0 \text{ or } -0.2 f_p \quad \text{for } \varepsilon_{ci} < \varepsilon_p < 0 \tag{3.6}$$

Where,

$$Z_m = \frac{0.5}{\dfrac{3+0.29\left|f'\right|}{145\left|f_c'\right|-1000} \cdot \left(\dfrac{\varepsilon_o}{-0.002} \right) + \left(\dfrac{\left|f_{lat}\right|^{0.9}}{170} \right)^{+\varepsilon_p}} \quad \left(f_c \text{ and } f_{lat} \text{ in MPa} \right) \tag{3.7}$$

and f_{lat}, is summation of principal stresses, acting transversely to the direction under consideration:

$$f_{\mathrm{lat}} = f_{c1} + f_{c2} + f_{c3} - f_{ci} \le 0 \quad i = 1 \text{ or } 2 \tag{3.8}$$

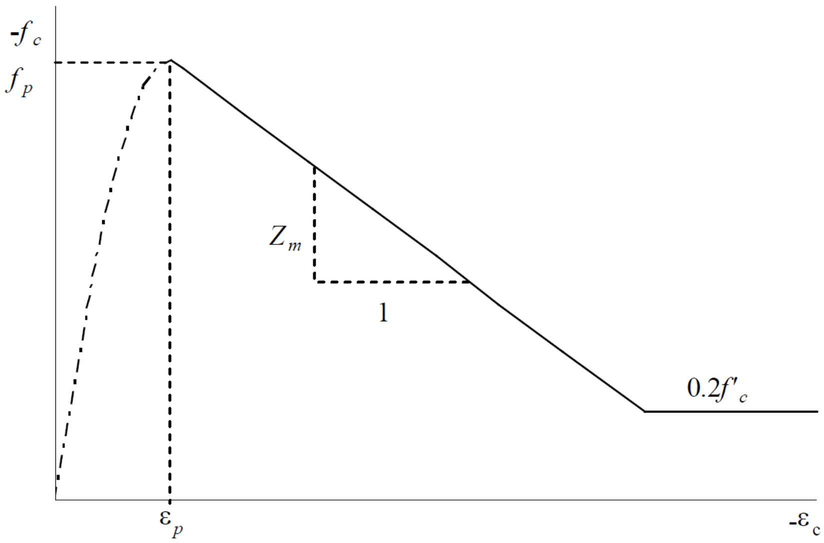

Figure 3-9 Modified Park-Kent post-peak concrete compression response

3.3.2.4.3 Compression Softening

Compression softening in cracked concrete is the reduction of compressive strength and stiffness, relative to the uniaxial compressive strength, due to coexisting transverse cracking and tensile straining. This reduction can be substantial and have considerable effects on the load-deformation response of reinforced concrete structures, in terms of stiffness, ultimate strength capacity and ductility.

In VecTor2, the compression softening is affected by a softening parameter, βd, with a value between zero and one, which is calculated by the compression softening models. In this study Vecchio 1992-A (e1/e2-Form) model is used, this strength-and-strained softened model is based on the results of 116 panel and shell element tests. The model also can take in to account for shear slip deformations. Both the uniaxial compressive strength and corresponding strain are softened.

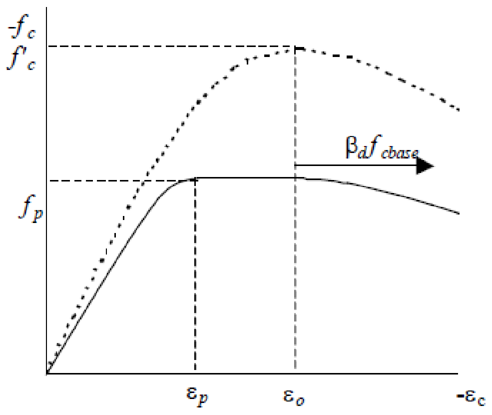

Figure 3-10 Strength and strain-softened compression response

3.3.2.5 Ductile Steel Reinforcement

For this study the reinforcement model of Bauschinger Effect (Seckin) is used. This reinforcement stress-strain response is composed mainly of three parts, as shown in Figure 3-11, including an initial linear-elastic response, a yield plateau, and nonlinear strain hardening phase until rupture. The reinforcement stress, fs, in tension and compression is determined as follows:

$$f_s = \begin{cases} E_s \varepsilon_s & \text{for } \varepsilon_s \leq \varepsilon_y \\ f_y & \text{for } \varepsilon_y < \varepsilon_s \leq \varepsilon_{sh} \\ f_u + \left(f_y - f_u\right)\left(\dfrac{\varepsilon_u - \varepsilon_s}{\varepsilon_u - \varepsilon_{sh}}\right)^P & \text{for } \varepsilon_{sh} < \varepsilon_s \leq \varepsilon_u \\ 0 & \text{for } \varepsilon_u < \varepsilon_s \end{cases} \tag{3.9}$$

where ε_s is the reinforcement strain ($\varepsilon_s=|\varepsilon_s|$), ε_y is the yield strain, ε_{sh} is the strain at the onset of the strain hardening, ε_u is the ultimate strain, Es is the elastic modulus, f_y is the yield strength, fu is the ultimate strength, and P is the strain-hardening parameter.

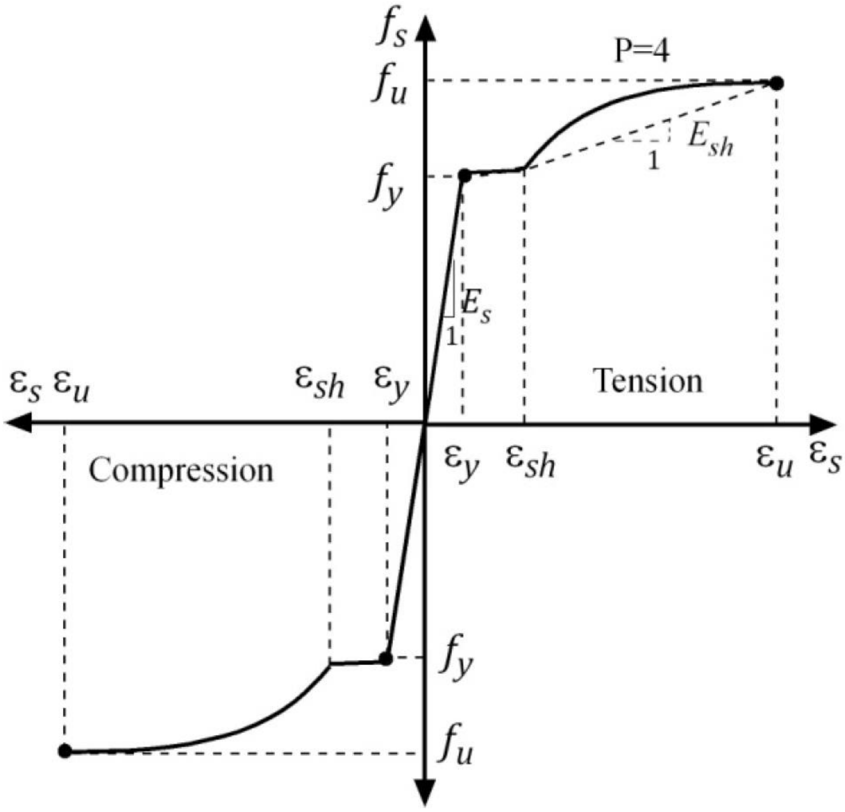

Figure 3-11 Ductile steel reinforcement stress-strain response [Nonlinear strain-hardening]

Table 3-3 Summary of concrete constitutive models

Material Property	Analytical Model
Concrete Compression Pre-Peak	Response Popovics (HSC)
Concrete Compression Post-Peak	Modified Park-Kent
Concrete Compression Softening Model	Vecchio 1992-A (e1/e2-Form)
Concrete Tension Stiffening Model	Bentz 2005
Concrete Tension Softening	Linear
Concrete Confinement Strength	Kupfer / Richart Model
Concrete Cracking Criterion	Mohr-Coulomb (Stress)
Concrete Crack Slip Check	Vecchio-Collins 1986

Concrete Crack Width Check	Agg./2.5 Max Crack Width
Concrete Creep and Relaxation	Not considered
Concrete Hysteretic Response	Nonlinear w/ Plastic Offsets
Reinforcement Hysteretic Response	Seckin Model (Bauschinger)
Reinforcement Buckling	Akkaya 2012
Reinforcement Dowel Action	Tassios Model (Crack Slip)
Concrete Bond	Eligehausen Model, Perfect Bond

3.3.3 Modelling of Geometry

The shear critical frame tested by Kien Vinh Duong at the University of Toronto, is modelled using the basic version of Vector2 as shown in Figure 3-12. A two-dimensional geometry is provided in the software to recreate the Duong frame. The geometry of the frame along with its reinforcement layout is shown on the figure below.

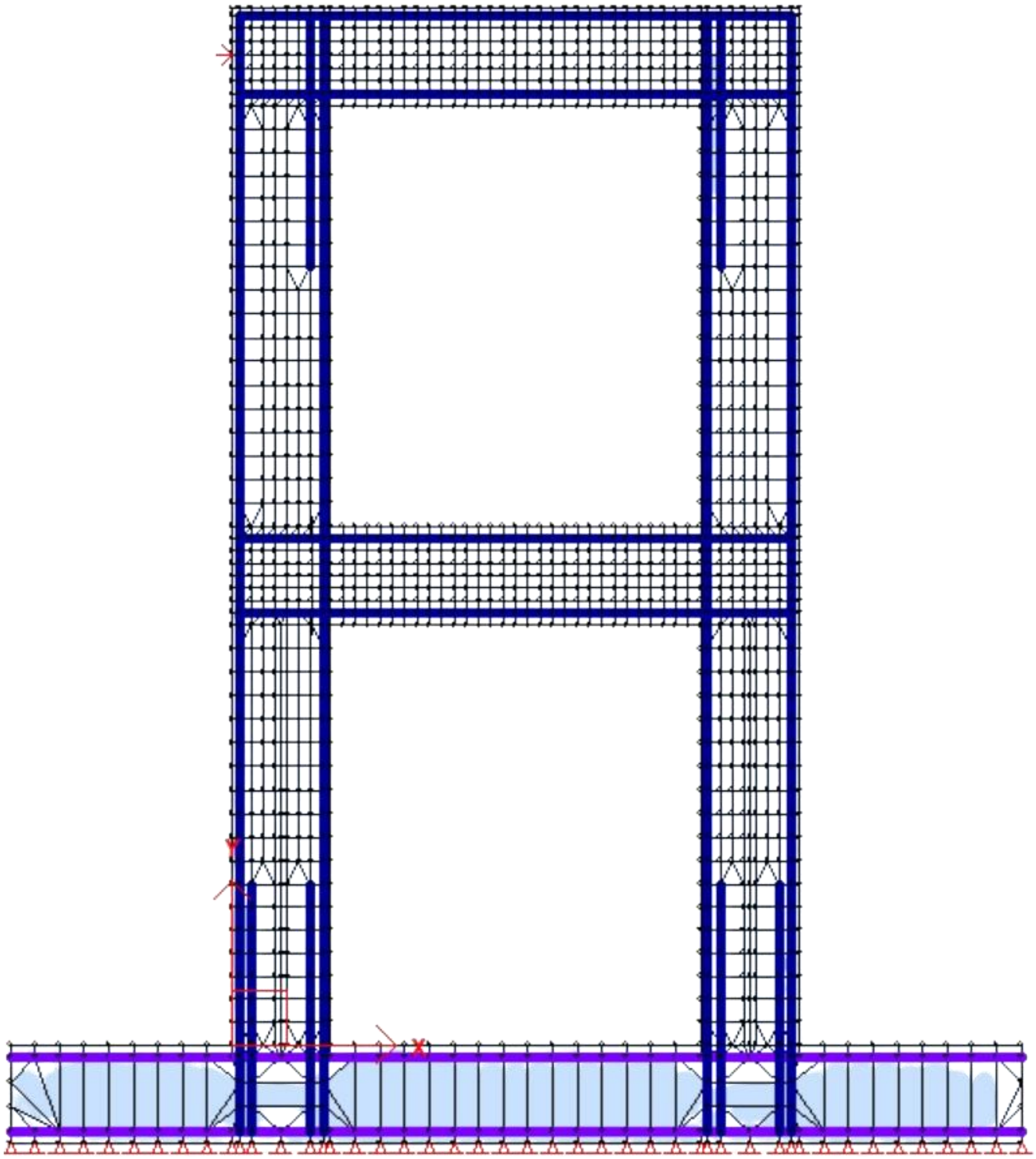

Figure 3-12 Geometry of the Duong frame model

3.3.4 Creating mesh

The mesh in Vector2 is created during modelling and it was created automatically when defining the ‘regions’ in the finite element model. Since the basic version of the software was used for this study the number of nodes and elements were limited to 3500 and 4000 respectively.

To comply with the aforementioned limitation an element size of 50mmx50mm was used for the beams, where failure is expected, while other regions such as columns and base were meshed using larger elements of size 100mmx100mm.Furthermore the interior of the base was not discretised as base failure is not expected.

3.3.5 Support Conditions

In the experimental setup, the concrete frame base was post-tensioned onto the strong floor to provide a fixed support via twelve floor bolts. There were six sets of bolts (two bolts per set) located along the base. Each bolt was stressed to approximately 35.5 kN or 71 kN per two bolts. These posttensioning forces were accounted for in the FE modelling by applying six 71 kN downwards forces at the bolt locations(refer to Figure 3-13).

In the model restraints were provided at all nodes along the base, in total 46 pinned supports were provided to restrain X and Y direction movement. This is justified by the experimental results that showed the base did not slide during testing, and stayed intact with little damage and with minimal uplift during testing.

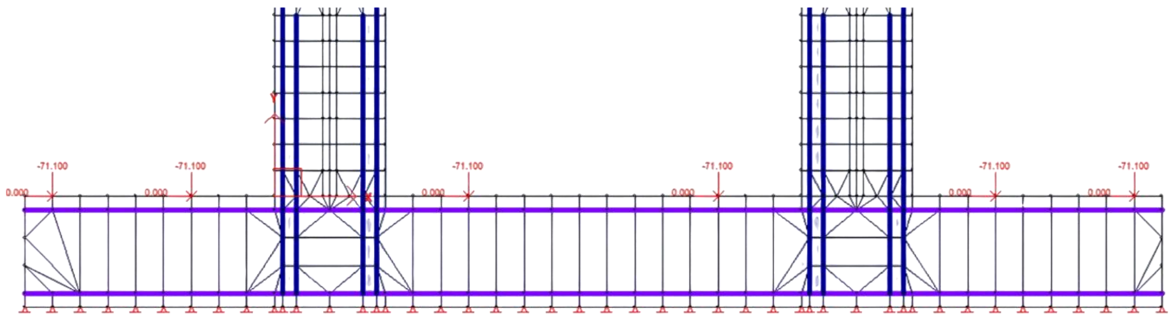

Figure 3-13 Support Conditions of the Duong frame model

3.3.6 Loading Conditions

A vertical column load of 420 kN was applied uniformly to the top of each column via a loading plate during the experiment of the Doung frame. In the FE modelling, this load was applied by distributing it to four nodes situated at the top of each column were each assigned 105 kN of vertical downward force that was held throughout the analysis (refer to Figure 3-14). The lateral load was applied at the mid-depth of the second-storey beam, in a displacement-controlled manner at 1 mm displacement increments throughout the analysis.

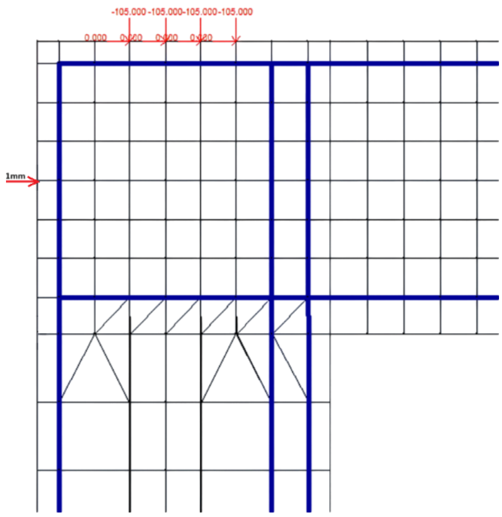

Figure 3-14 Loading Conditions of the Duong frame model

3.4 Modelling and Analysis with Seismostruct

3.4.1 Introduction to Seismostruct

SeismoStruct is a Finite Element package for structural analysis, capable of predicting the large displacement behavior of space frames under static or dynamic loadings, taking into account both geometric nonlinearities and material inelasticity. SeismoStruct features a nonlinear analysis solver capable of using both distributed plasticity and plastic hinge models. Its accuracy is well demonstrated by numerous test prediction exercises.

SeismoStruct allows for accurate estimation of damage accumulation via the spread of inelasticity along the member length and across the section depth. Performance criteria can also be set, allowing the user to identify the instants at which different performance limit states are reached. The sequence of cracking, yielding, failure of members throughout the structure can also be, in this manner readily obtained.

3.4.2 Material modelling

In this study distributed inelasticity elements are used to model the test frame, Doung frame. These elements are becoming widely employed in earthquake engineering applications, either for research or professional engineering purposes due to their advantages when compared to the simpler lumped-plasticity models. Distributed inelasticity elements do not require calibration of empirical response parameters against the response of an actual or ideal frame element under idealized loading conditions, as is instead needed for concentrated-plasticity models.

Such models feature additional assets, which can be summarized as: no requirement of a prior moment-curvature analysis of members; no need to introduce any element hysteretic response (as it is implicitly defined by the material constitutive models); direct modelling of axial load-bending moment interaction (both on strength and stiffness); straightforward representation of biaxial loading, and interaction between flexural strength in orthogonal directions.

3.4.2.1 Constitutive Models for Concrete

In this study the constitutive model chosen for concrete is that of Mander's. This is a uniaxial nonlinear constant confinement model, that follows the constitutive relationship proposed by Mander et al. [1988] and the cyclic rules proposed by Martinez-Rueda and Elnashai [1997]. The confinement effects provided by the lateral transverse reinforcement are incorporated through the rules proposed by Mander et al. [1988] whereby constant confining pressure is assumed throughout the entire stress-strain range.

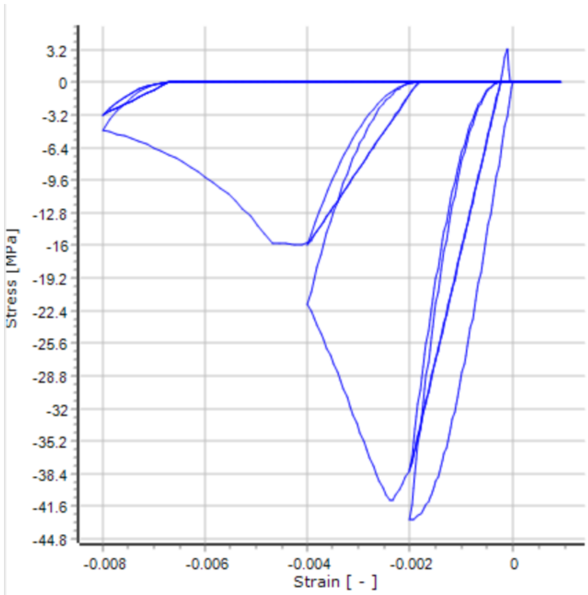

Figure 3-15 Concrete stress vs strain curve

3.4.2.2 Constitutive Models for Reinforcement

In this study the constitutive model chosen for Reinforcement is that of Menegotto-Pinto steel model. This is a uniaxial steel model based on a simple, yet efficient, stress-strain relationship proposed by Menegotto and Pinto [1973], coupled with the isotropic hardening rules proposed by Filippou et al. [1983]. The current implementation follows that carried out by Monti et al. [1996]. Its employment should be confined to the modelling of reinforced concrete structures, particularly those subjected to complex loading histories, where significant load reversals might occur. As discussed by Prota et al. [2009], with the correct calibration, this model, initially developed with ribbed reinforcement bars in mind, can also be employed for the modelling of smooth rebars, often found in existing structures.

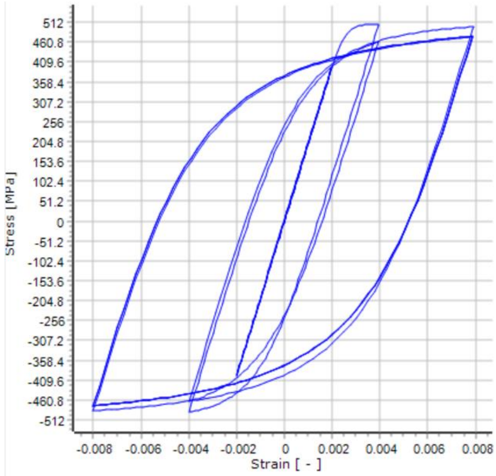

Figure 3-16 Reinforcement stress vs strain curve

3.4.3 Modelling of Geometry

In this study a model of the Doung frame was done on SeismoStruct as shown in Figure 3-17.

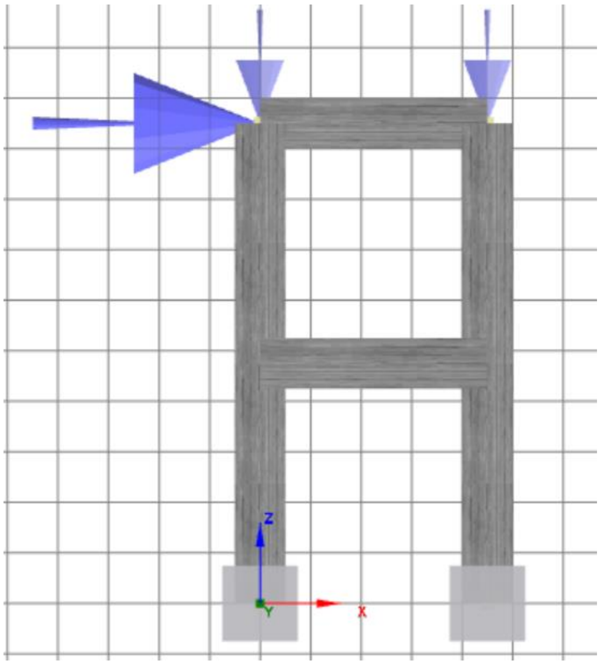

Figure 3-17 Modelling of Geometry

Geometric nonlinearity including large displacement and P-Delta effects are taken into account in SeismoStruct, through the employment of a total co-rotational formulation developed and implemented by Correia and Virtuoso [2006]. The implemented total co-rotational formulation is based on an exact description of the kinematic transformations associated with large displacements and three-dimensional rotations of the beam-column member. This leads to the correct definition of the element's independent deformations and forces, as well as to the natural definition of the effects of geometrical non-linearities on the stiffness matrix.

3.4.4 Creating mesh

In SeismoStruct , use is made of the so-called fibre approach to represent the cross-section behavior, where each fibre is associated with a uniaxial stress-strain relationship; the sectional stress-strain state of beam-column elements is then obtained through the integration of the nonlinear uniaxial stress-strain response of the individual fibres in which the section has been subdivided (the fiber modelling of a typical reinforced concrete cross-section is depicted, as an example, in figure 3-18). Such models feature additional assets, which can be summarized as: no requirement of a prior moment-curvature analysis of members; no need to introduce any element hysteretic response (as it is implicitly defined by the material constitutive models); direct modelling of axial load-bending moment interaction (both on strength and stiffness); straightforward representation of biaxial loading and interaction between flexural strength in orthogonal directions.

The sectional stress-strain state of beam-column elements is then obtained through the integration of the nonlinear uniaxial stress-strain response of the individual fibres (typically 100-150) in which the section has been subdivided (the discretisation of a typical reinforced concrete cross-section is depicted, as an example, in the figure below).

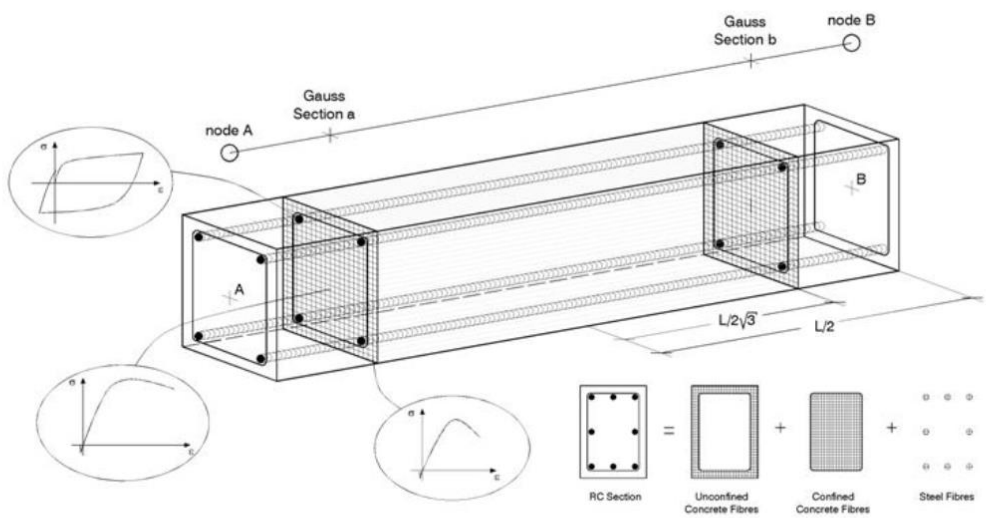

Figure 3-18 Fiber modelling in SeismoStruct

In this study meshing in SeismoStruct was done at Element level through element subdivision and at a section level through the use of Fibers. The number of section fibres used in equilibrium computations carried out at each of the element's integration sections needs to be defined. The ideal number of section fibres, sufficient to guarantee an adequate reproduction of the stress-strain distribution across the element's cross-section, varies with the shape and material characteristics of the latter, depending also on the degree of inelasticity to which the element will be forced to.

As a crude rule of thumb, SeismoStruct recommends users to consider that single-material sections will usually be adequately represented by 100 fibres, whilst more complicated sections, subjected to high levels of inelasticity, will normally call for the employment of 200 fibres or more. In our modelling the number of section fibre used were 152 for each reinforced concrete section.

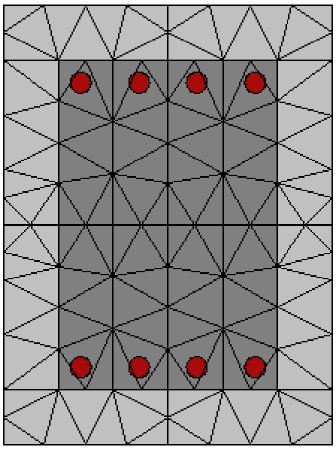

Figure 3-19 Section discretization via fibers

At the element level an integration section of 5 sub-element was utilized to subdivide each element into five.

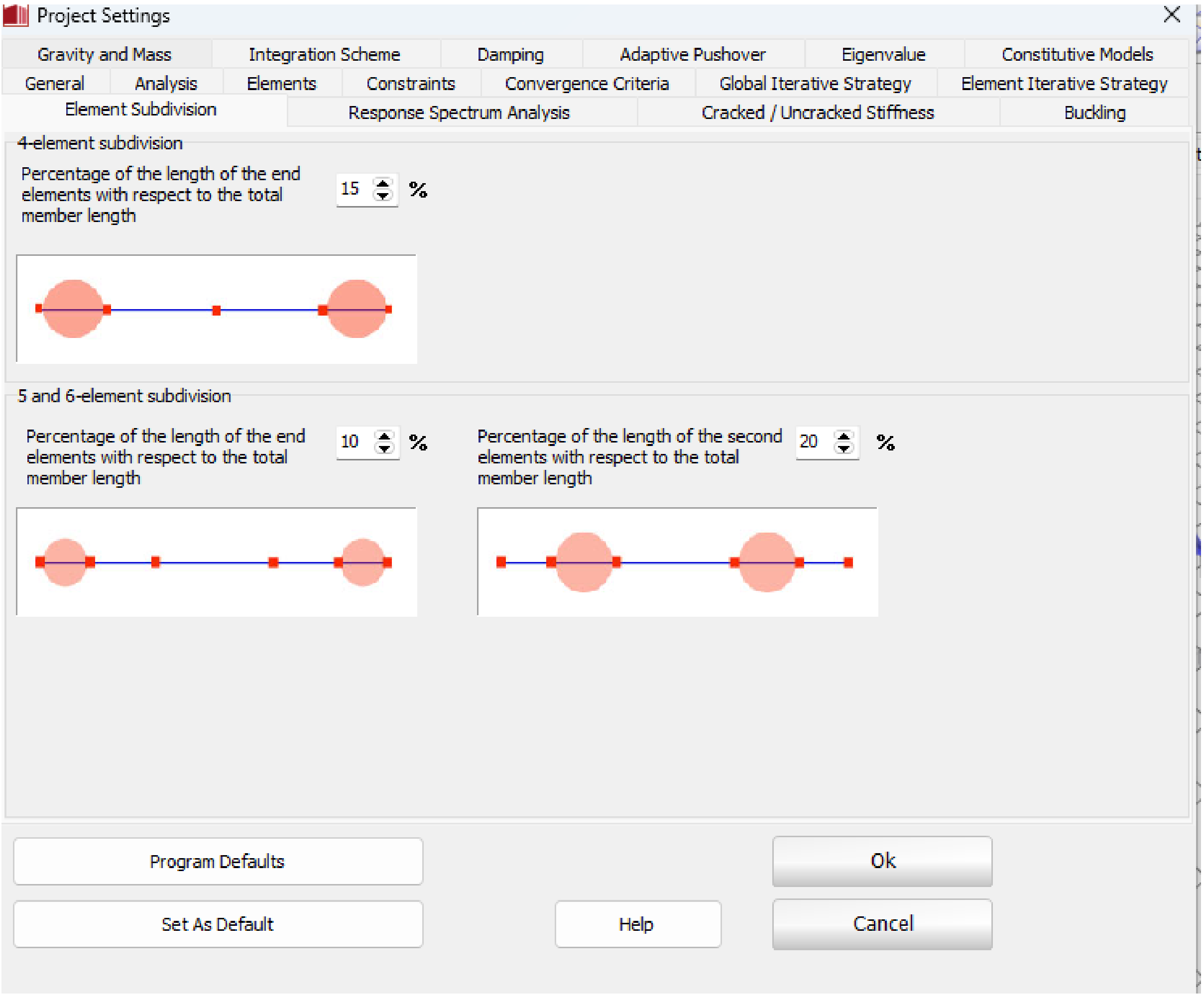

Figure 3-20 Element subdivision

3.4.5 Support & Loading Conditions

As shown in Figure 3-17, the frame support was modelled as fixed at both column bases. The constant load of 420KN was directly applied on top of each column to simulate the test vertical load. As for the horizontal load two pushovers based on Force controlled and displacement-controlled procedures were conducted, one applying the load in a displacement-controlled manner while the other was applied in a force-controlled manner.

3.5 Modelling and Analysis with ETABS

3.5.1 Introduction to ETABS

ETABS is a comprehensive finite element analysis package from Computers and Structures Inc. for structural analysis and design. It is probably the most widely used analysis tool among the easily available analysis software for building structures. It can perform linear-elastic static, dynamic and time-history analyses for wide variety of materials. Nonlinear static and time-history analyses can be carried out using either a lumped or distributed nonlinearity models.

The software possesses a versatile and user-friendly graphical interface as well as a fast and powerful analysis engine. Both structure creation and the result visualization are conveniently done through the graphical interface. Therefore, it is highly suited for practical everyday use by office design engineers. The version of ETABS used in this study is V20.1.0 that was released on 31-March-2022.

3.5.2 Material modelling

3.5.2.1 Constitutive Models for Concrete

In this study the constitutive model chosen for concrete is that of Mander's. This is a uniaxial nonlinear constant confinement model, that follows the constitutive relationship proposed by Mander et al. [1988]. Figure 3-21 the actual concrete stress vs strain curve used in the ETABS modeling of the Doung frame.

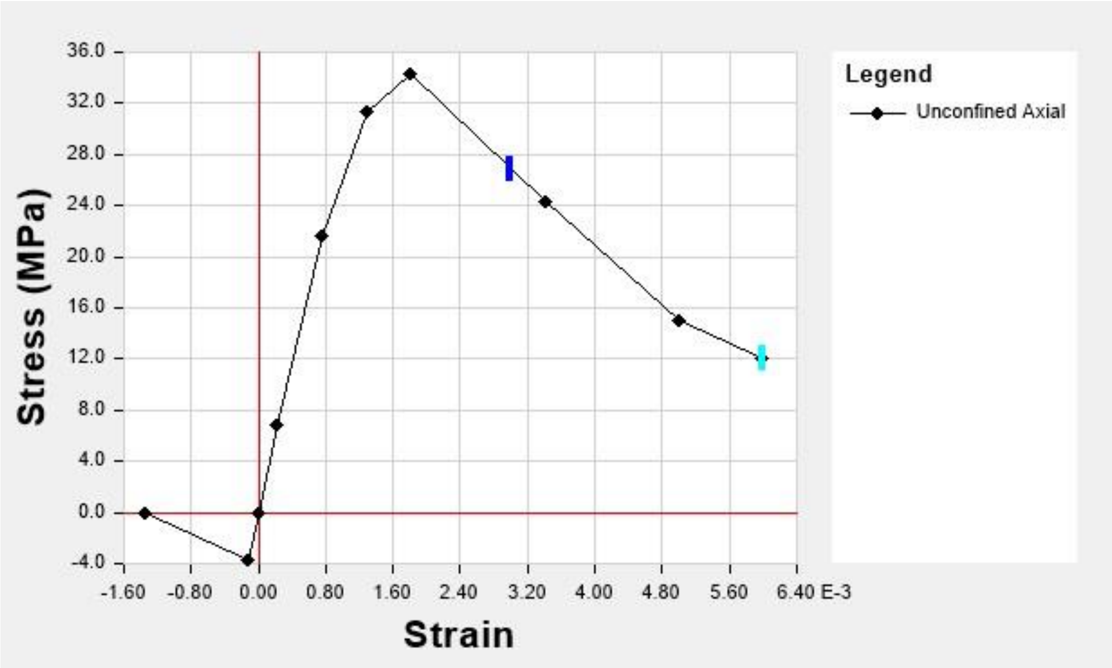

Figure 3-21 Concrete stress vs strain curve

3.5.2.2 Constitutive Models for Reinforcement

In this study the material chrematistics values from actual test (Refer Table3-3) conducted on reinforcements used in the Duong were entered in to the program and the following reinforcement stress vs strain curve was generated automatically.

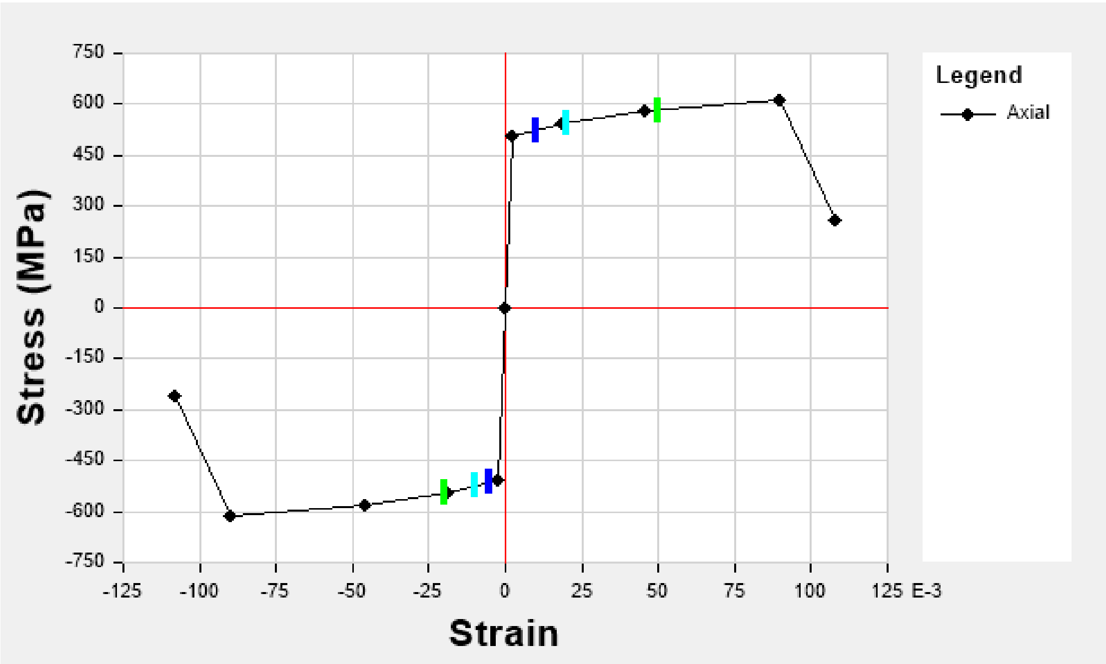

Figure 3-22 Reinforcement stress vs strain curve

3.5.3 Modelling of Geometry

In this study a model of the Doung frame was done on ETABS as if it were a linear-elastic static analysis problem. In order to generate automatic hinges, longitudinal reinforcement details should be defined including bar sizes, locations, and yield strengths. However, for sections with unsymmetrical reinforcement arrangement modelling using custom section designer is required.

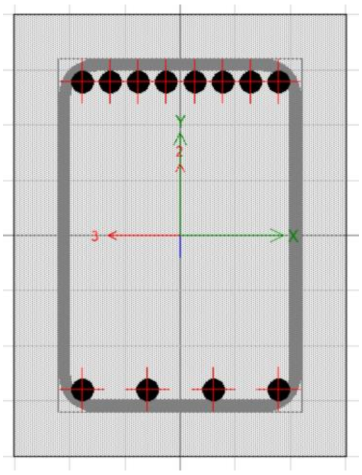

Figure 3-23 Modelling using Section Designer

After material modelling, sectional modelling, definition of geometry, assignment of frame and hinge properties the resulting model is as follows;

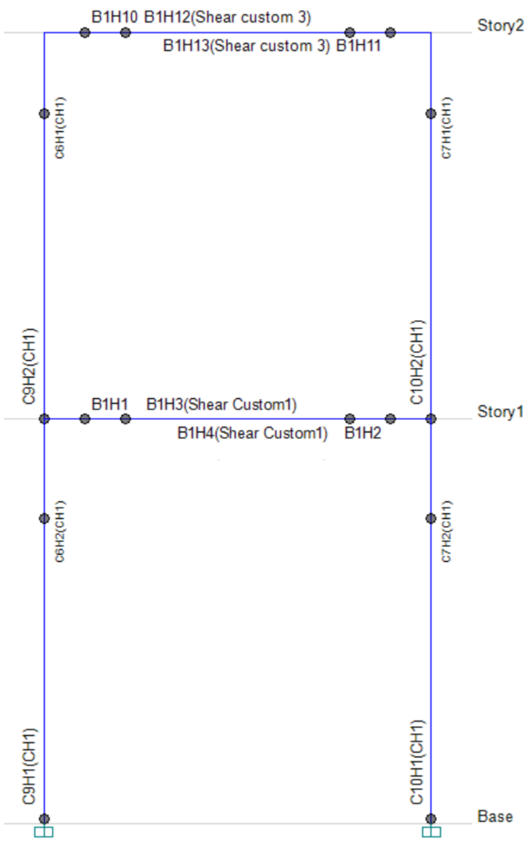

Figure 3-24 Modelling of Geometry and Hinge Definitions

3.5.4 Hinge definitions

In this study both lumped and distributed nonlinearity models are used to model the test frame, Doung frame. The distributed nonlinearity elements are utilised using fiber (P-M2-M3) hinges for columns. While lumped plasticity models are used to define moment and shear hinges at the beams.

The next step is to assign hinges to desired locations. This is one of the most critical phases in the nonlinear modelling process with ETABS. Both hinge locations and selected hinge properties have great influence on the response computed. For the moment hinges, the use of a hinge length in the range of cross section depth, h, is a generally accepted approach (CSI, 2005); therefore, a hinge length of h is used for the moment hinges throughout this study. For modelling moment hinges in ETABS tables in ASCE 41-13 with EC8 2005, Part 3 Acceptance Criteria were chosen to generate Auto M3 hinges.

For the selection of the shear hinge length, on the other hand, there is much less information available in the literature. In this study, 1.5 times of the cross-section depth is used for the shear hinge length as per the recommendation of Serhan Güner (2008) [6].

The definition of the shear hinges will follow two separate approaches, default and custom hinge definitions. For the custom definitions the specialty support software Response 2000 will be used to generate hinge Stress-Strain Curves.

3.5.4.1 *Steps in defining custom hinges*

- Identify the possible locations where shear hinges may be required,
    - The shear capacity of the beam and column sections at locations of maximum shear force were hand calculated as 189 KN for the beams and 709 KN for the columns. The detail calculations are attached on Appendix A. Response 2000 gave the shear capacities as 225 KN for the beams and 721 KN for the columns.
    - From a preliminary analysis of the frame, it was found that the expected maximum shear force on frame is 227 KN for the beams and 215 KN for the columns. This shows that nonlinear hinge is only necessary for the beams.
    - The hinge locations are as shown in Figure 3-24;
- Model the section in Response 2000, this will be done at all sections where a shear hinge is required.

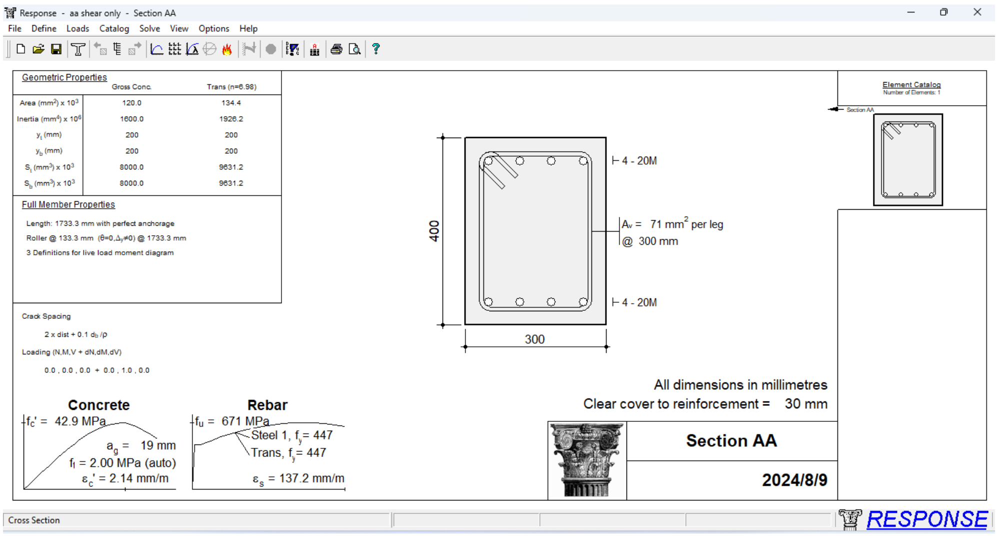

Figure 3-25 Sectional modelling in Response 200

- Run a linear elastic analysis in ETABS to find the relative ratios of axial load, bending moment and shear force at the section in question, this will be the loading condition in Response 2000. The ratio of the moment to shear force at the section of the hinge location is inputted as a loading condition to consider moment-shear interaction in the sectional response.

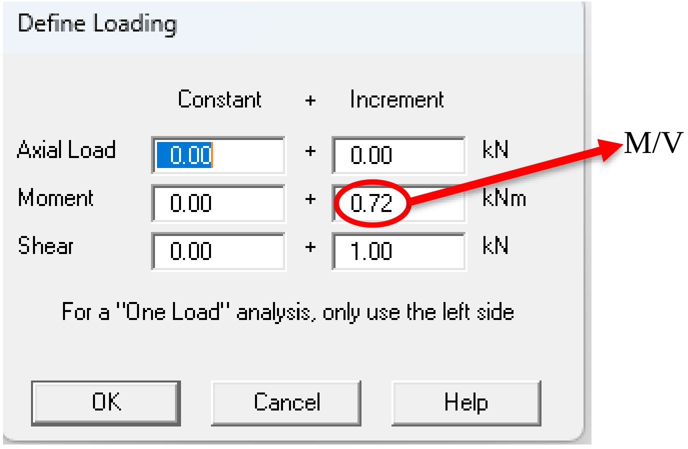

Figure 3-26 Sectional loading in Response 2000

- Run the solve sectional responses command on Response 2000, to get shear force vs shear strain and other results

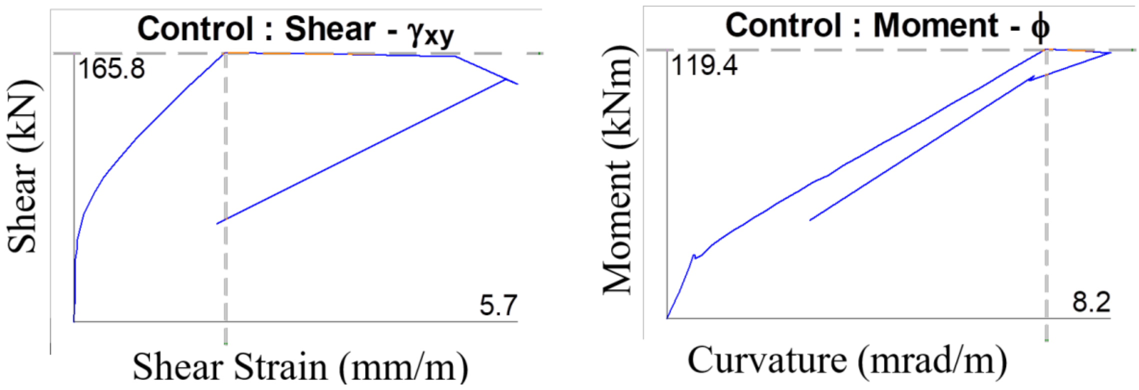

Figure 3-27 Sectional responses

- Export the data and convert it to average shear stress vs shear strain, use effective cross-sectional depth to calculate the area (A_{eff}=bd). (Shear stess= Shear Force/A_{eff})

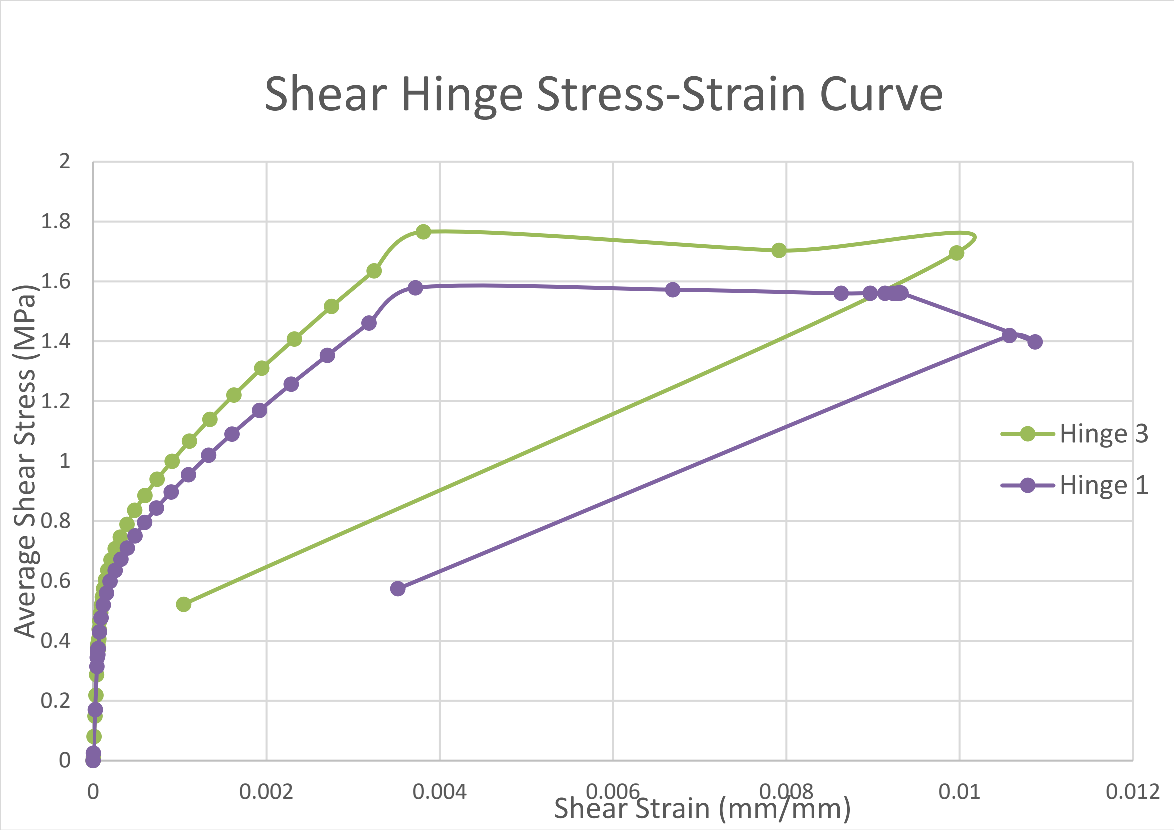

Figure 3-28 Shear Hinge Stress-Strain Curve

Note: In the above figure Hinge 1 represents first story beam hinges, Hinge 3 represents second story beam hinges.

- ETABS uses normalized stress-strain curves in its definition of shear hinges so normalize the results with the yield stress and strain values
- Input these values in ETABS at each shear hinge location (as shown in Figure 3-29)
- Run analysis and repeat until the loading condition used in Response 2000 and the internal forces after the analysis converge

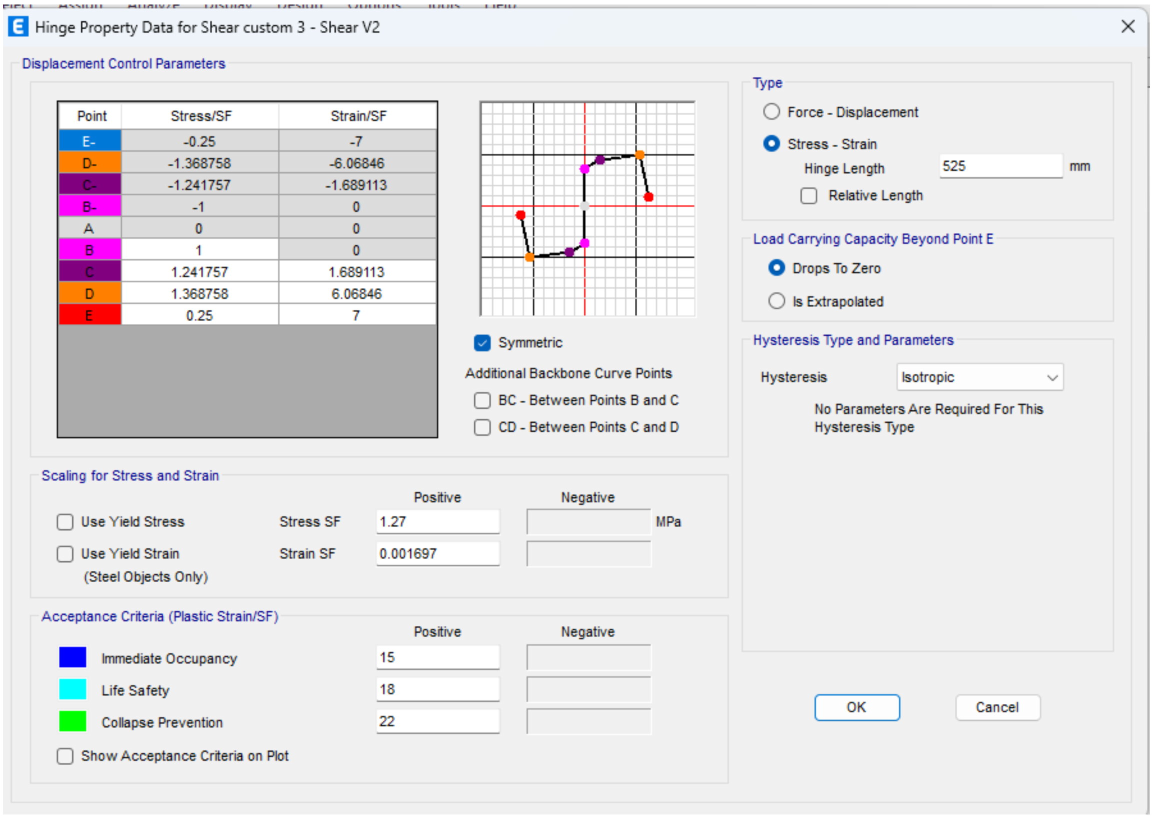

Figure 3-29 Custom shear hinge definition in ETABS

3.5.5 Support & Loading Conditions

As shown in the above figure, Figure 3-24, the frame support was modelled as fixed at both column bases. The constant load of 420KN was directly applied on top of each column to simulate the test vertical load. As for the horizontal load pushover based on Force controlled procedure is conducted. The nonlinear procedure will start from an initial condition of gravity nonlinear load case.

CHAPTER 4 RESULTS AND DISCUSSION

4.1 Introduction

In this study several models of a shear critical reinforced concrete frame are analysed using three separate software, Vector2, Seismostruct and ETABS. The results and discussions presented here will be focused on the assessment of the accuracy of each model and software in predicting the performance of the shear critical frame. The detail collected result and the outline of the analysis procedure followed in this study are discussed in chapter three.

This section entails detailed discussions of the findings of our numerical study. Yield capacity, peak capacity, yield displacement, peak displacement, ductility, hinge formation and energy dissipation of the models will be examined using experimental data from Doung frame tested at the university of Toronto. Furthermore, the investigation extends by performing a comparative analysis of the results obtained from different models and software. This comparative analysis aims to assess the variations in peak lateral load capacity, peak displacement, and other parameters among different models. A assessment on the proposal for generating custom shear hinges in ETABS will be conducted as compared to default hinges.

4.2 Results and discussion

In this study examines and compares results from all three software and six models. The models are as follows;

- Vector2 Model
- Seismostruct Model
- ETABS Models
    - No shear hinge
    - Default shear hinge
    - Custom shear hinge

4.2.1 Vector2 Model

4.2.1.1 Pushover curve

Figure 4-1 illustrates the lateral load versus second-story displacement for both the analytical and experimental responses. Although, Vector2 predicted a slightly greater peak load (376 KN) than the experimental result (327 KN) this is within a good accuracy as a deviation of 15.12% is acceptable in shear critical structure. Additionally, the FE program also predicted a higher initial stiffness than that of the experimental result.[6]

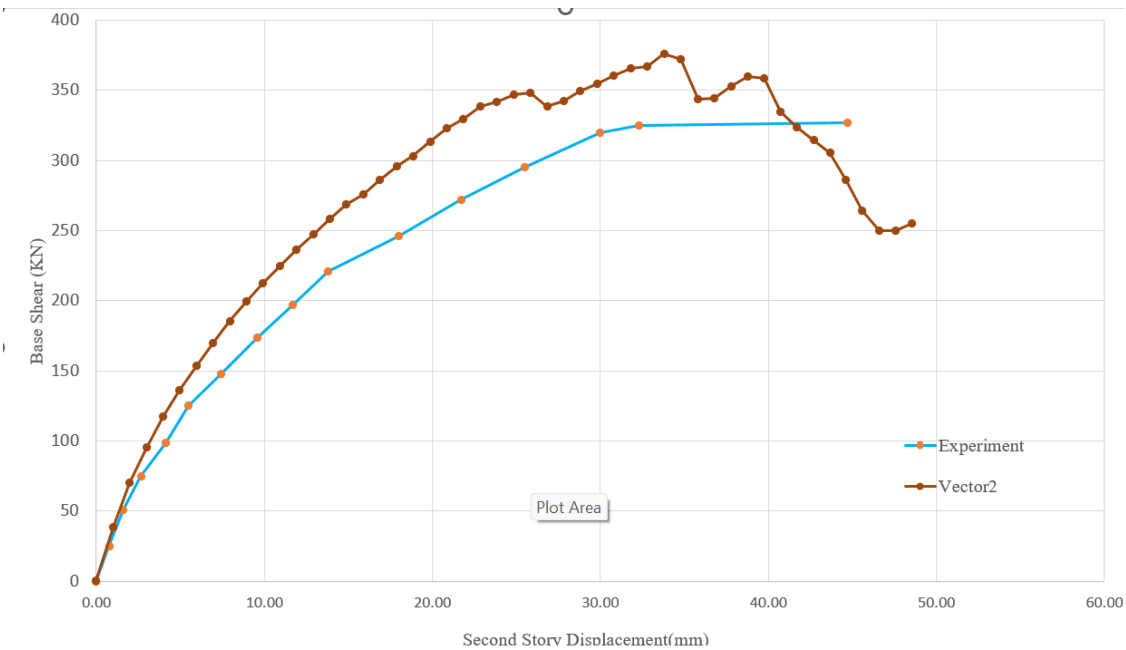

Figure 4-1 Pushover curve Vector2

The displacement at peak load was 33.79 mm for the Vector2 model, which is less than the experimental result of 44.7 mm. However, in the experiment the peak load and the peak displacement coincided while the analytical model predicts the maximum deflection of 48.56 mm at the end of descending branch of the pushover curve.

4.2.1.2 Failure mode

Figure 4-2 illustrates the cracking pattern for the analytical result at a top story displacement of 33.79 mm. It can be observed from the thick crack lines that both first and second story beams are suffering shear cracks with failure imminent.

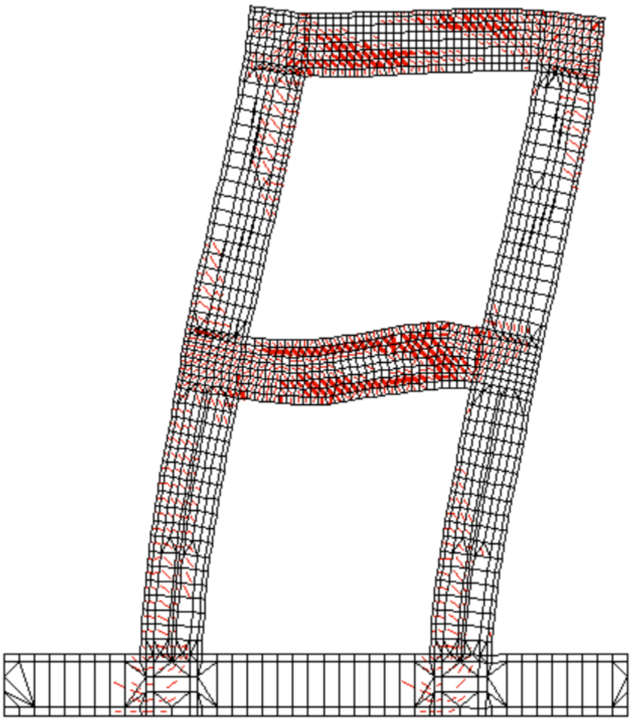

Figure 4-2 Deformed shape and crack pattern

Taking a closer look at the first story beam and compare to a photo at a similar stage of the experiment, there is a strong correlation with respect to both crack width and cracking direction for the right side of the beam, however the model fails to replicate the left side cracking by entering the descending branch of the pushover curve

.

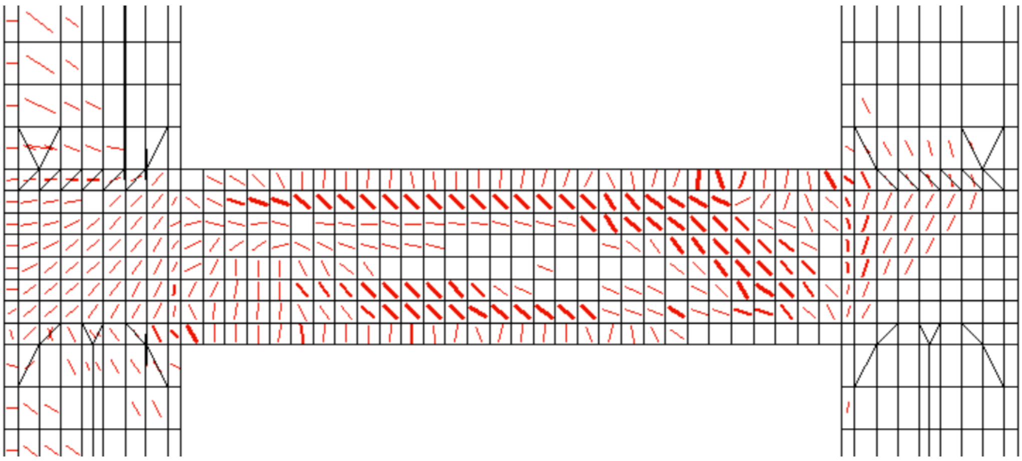

a) FE model cracking pattern of first story beam

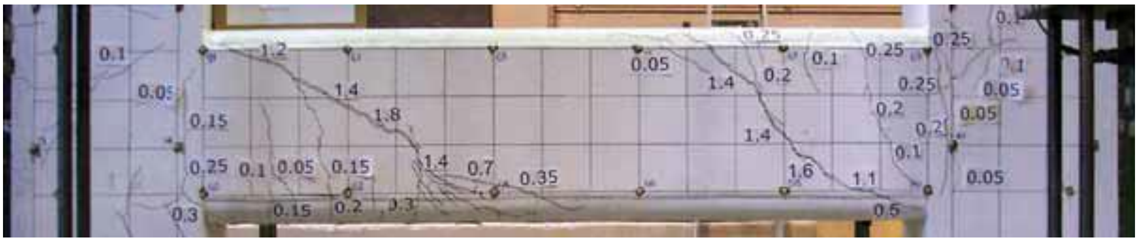

b) Experimental cracking pattern of first story beam

Figure 4-3 FE model vs Experimental cracking pattern of first story beam

We can also examine the stress state of both longitudinal and transverse (smeared) reinforcement. Figure 4-4 shows the stress in longitudinal reinforcement(truss) and Figure 4-5 shows the stress in transverse reinforcement (smeared).

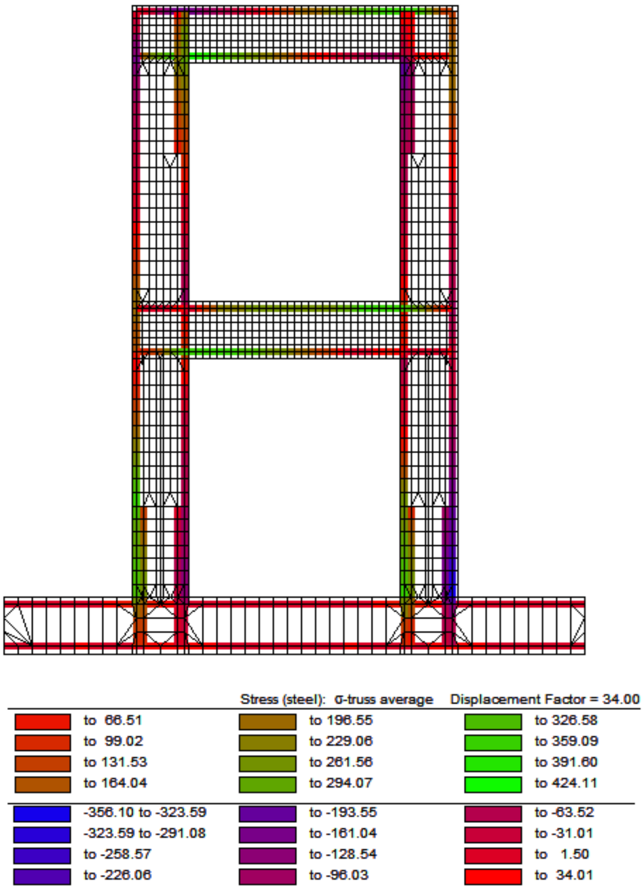

Figure 4-4 stress in longitudinal reinforcement(truss)

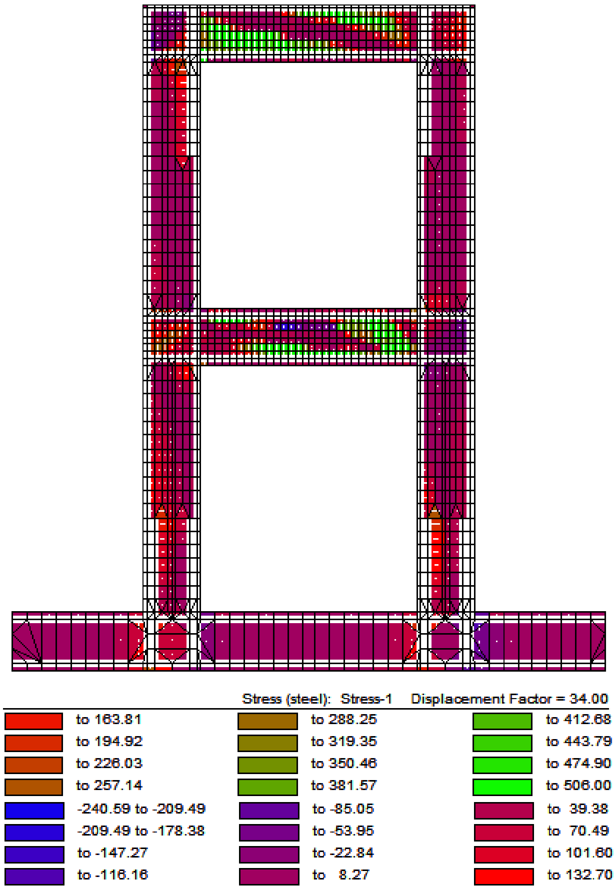

Figure 4-5 stress in transverse reinforcement (smeared)

It can be seen from that longitudinal reinforcement yielding has occurred, and some transverse reinforcement also has yielded. This indicates a combined flexural-shear mechanism, a similar failure mode to that of the experiment.

Overall, from the above discussion it's fair to conclude that even the basic version of Vector2 is capable of predicting accurately shear critical behavior.

4.2.2 Seismostruct Model

4.2.2.1 Pushover curve

Figure 4-6 illustrates the lateral load versus second-story displacement for both the analytical and experimental responses. Seismostruct predicted a slightly greater peak load (344 KN) than the experimental result (327 KN) this is a highly accurate estimate with a small deviation of 5.19%. Additionally, the FE program also predicted a slightly higher initial stiffness than that of the experimental result.

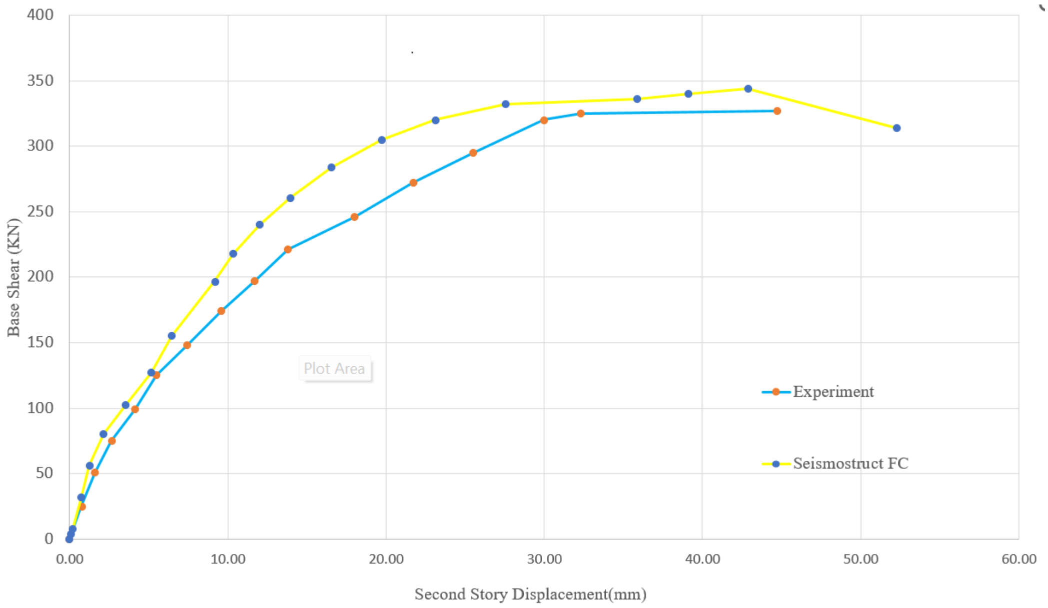

Figure 4-6 Pushover curve Seismostruct

The displacement at peak load was 42.9 mm for the Seismostruct model, which is slightly less than the experimental result of 44.7 mm. However, in the experiment the peak load and the peak displacement coincided while the analytical model predicts the maximum deflection of 52.3 mm at the end of descending branch of the pushover curve.

4.2.1.2 Failure mode

Figure 4-7 illustrates hinge formation pattern for the analytical model, this is done based on the performance requirements and compliance criteria set forth in Eurocode 8, part 3. Accordingly three criterion for code based checks were defined namely;

- moment(Green), and
- shear(Red).

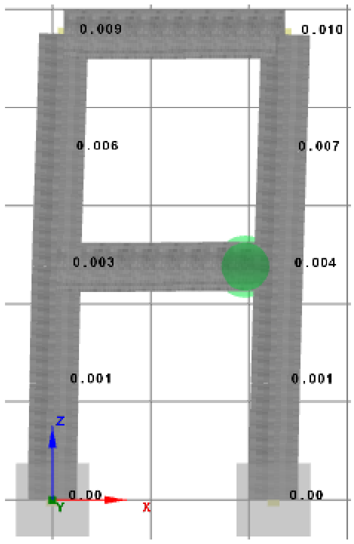

V=196 KN $\Delta_{2nd\ story}$=9.18mm

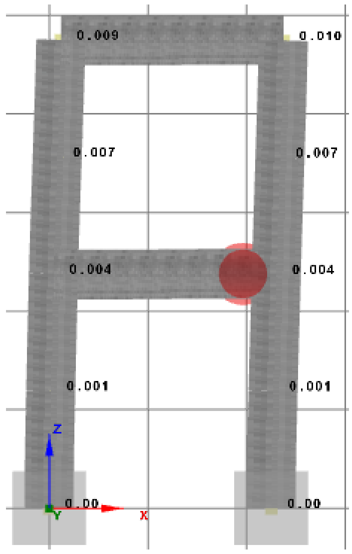

V=200 KN $\Delta_{2nd\ story}$=9.42mm

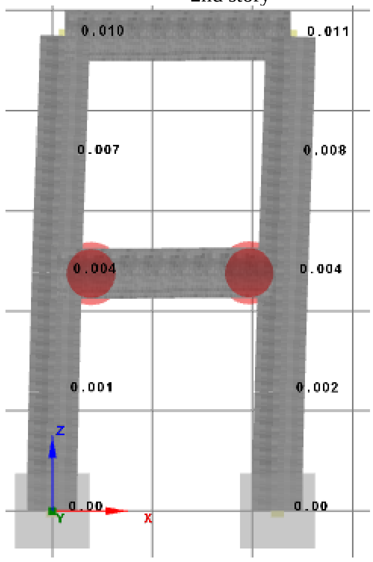

V=212 KN $\Delta_{2nd\ story}$=10.1mm

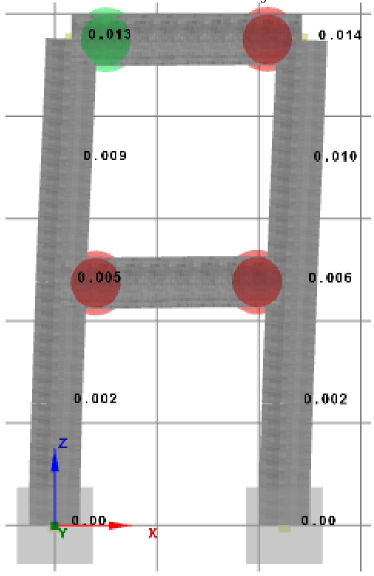

V=252 KN $\Delta_{2nd\ story}$=13.1 mm

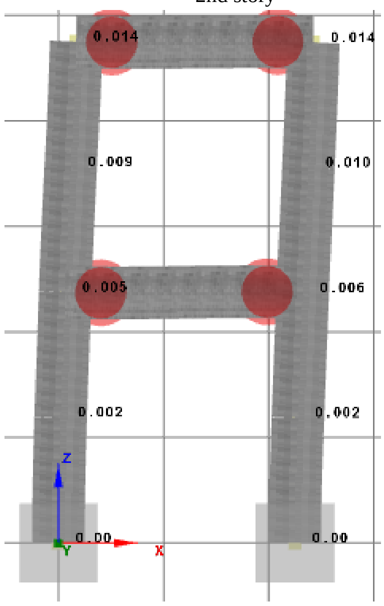

V=256 KN $\Delta_{2nd\ story}$=13.4 mm

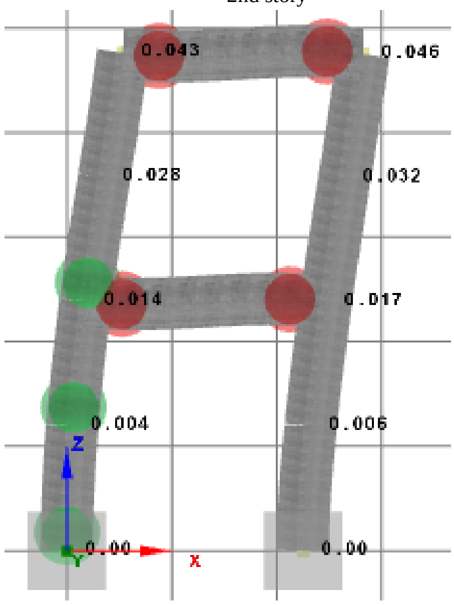

V=344 KN $\Delta_{2nd\ story}$=42.86 mm

Figure 4-7 Code based checks on the Doung frame model

A quick look at Figure 4-7shows that the first story beam starts to fail by combined moment and shear mechanism as both failures occur almost simultaneously at a base shear of 196 KN and 200 KN. Since the capacity of the section for both pure shear (225 KN) and pure moment (189 KNm) is not yet reached, it indicates that a combined failure mode of flexure and shear has occured. Hence a failure mode of flexural-shear is predicted, a similar failure mode to that of the experiment.

Seismostruct allows for users to monitor the state of stress/strain at any point in the sections discretized via fibers. Taking advantage of this feature we have selected top and bottom reinforcement fibers at each side of the beams for both first and second story beams. Table 4-1 shows the stress state of longitudinal reinforcement at the selected locations.

Table 4-1 Longitudinal reinforcement state of stress

Base Shear (KN)	Longitudinal Reinforcement stress (MPa)							
	First Story beam				Second Story beam			
	Left end Top Reinf.	Left end Bottom Reinf.	Right end Top Reinf.	Right end Bottom Reinf.	Left end Top Reinf.	Left end Bottom Reinf.	Right end Top Reinf.	Right end Bottom Reinf.
0	-0.07	0.12	-0.07	0.02	0.33	-0.42	0.33	-0.42
52	-18.21	18.24	17.97	-2.54	-13.45	10.84	11.44	-14.05
100	-25.63	146.02	145.06	-3.00	-31.69	153.31	144.68	-30.30
152	-40.12	248.36	259.58	-4.80	-41.79	216.04	211.08	-41.05
200	-49.89	348.36	373.18	-5.91	-55.04	281.05	279.29	-54.77
240	-61.78	431.20	447.48	-6.07	-66.50	338.26	335.34	-66.04
252	-61.95	447.17	448.69	-2.47	-70.77	361.54	358.14	-70.24
292	-11.75	451.27	452.89	0.00	-78.61	447.41	442.75	-80.41
300	2.63	452.35	454.16	0.00	-65.64	448.65	447.81	-77.21

It can be seen from the above table that longitudinal reinforcement yielding first occurred at the top reinforcement of the right end of the first story beam at a base shear of 240 KN. Shortly after this the bottom reinforcement of the left end of the first story beam also yielded at a base shear of 252 KN. It should be noted that shear failure with ‘serious diagonal cracking’ has occurred at the first story beam at this stage. The second story longitudinal reinforcement also yielded in a similar manner at a base shear of 292 KN. This further substantiates that the failure mode is a combined flexural-shear mechanism.

Therefore, we can see that the SeismoStruct model gave accurate prediction of shear critical behavior in the test frame with close correlation to experimental data.

4.2.3 ETABS Models

In this study three different types of models were created on ETABS for the Doung shear critical frame. First the frame is analyzed using the widely used approach of using moment hinges only, then we will use the Default shear hinge option to examine its adequacy and finally we will create a user defined shear hinge assisted by the supporting specialty software Response 2000.

4.2.3.1 Pushover curve

Figure 4-8 shows the lateral load versus second-story displacement for all three ETABS models and experimental responses.

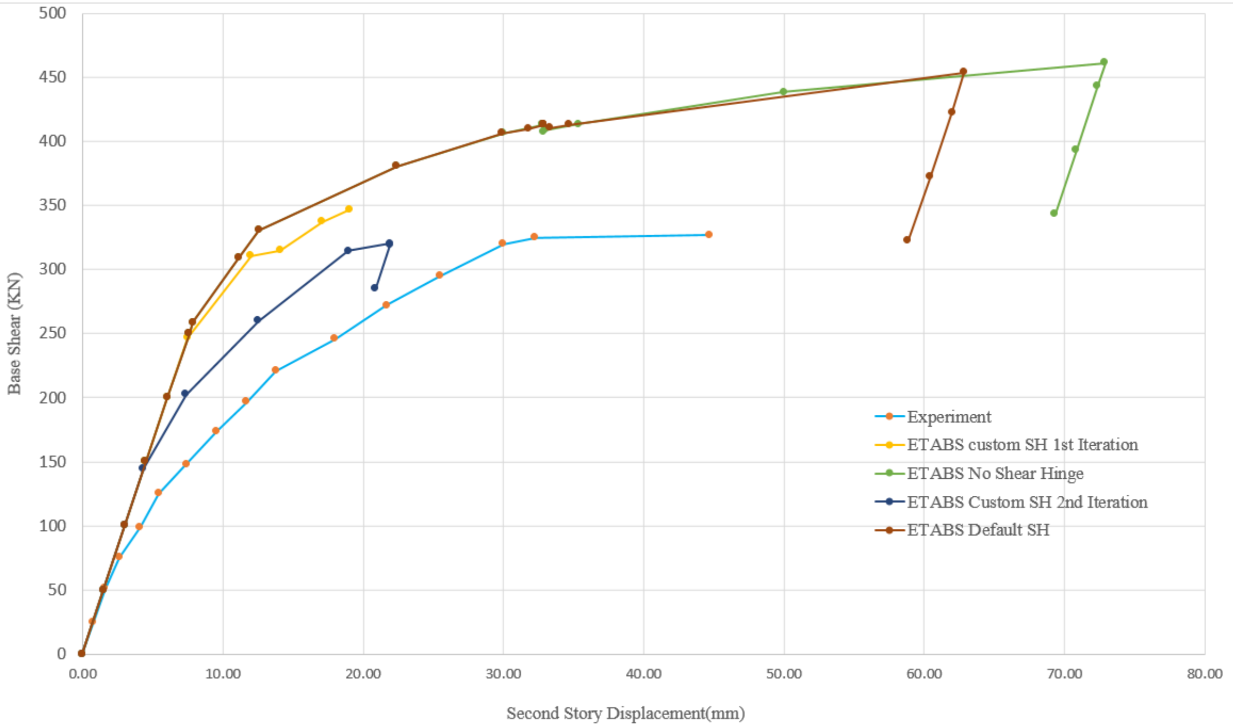

Figure 4-8 Pushover curve ETABS

The following can be noted from the above pushover curve;

- The ‘No shear hinge’ model predicted a much higher peak load (461.5 KN) than the experimental result (327 KN) which is a highly inaccurate estimate with a huge deviation of 41.1%. Additionally, this model also predicted a greater displacement capacity (72.9 mm) than that of the experimental result (44.7 mm). It can be seen from this that this approach is not accurate for the case of shear critical frame.

- The 'Default shear hinge' model predicted a higher peak load (453.84KN) than the experimental result (327 KN) which is inaccurate estimate with a deviation of 40.3%. However, this model predicted a relatively closer displacement capacity (62.86 mm) to that of the experimental result (44.7 mm). It can be concluded from this that while the use of the default shear hinge showed an improvement from the previous model this approach is still not accurate for the case of shear critical frame.
- The 'Custom shear hinge' model predicted a higher peak load (319 KN) than the experimental result (327.36 KN) this is a highly accurate estimate with a small deviation of -2.4%. However, this model also predicted a much smaller displacement capacity (21.91 mm) than that of the experimental result (44.7 mm). while this is a significant discrepancy it is on the conservative side. It can be concluded from this that this is the best approach of the three for the case of shear critical frame.

4.2.3.1 Failure mode

Figure 4-9 illustrates hinge formation pattern for the 'Custom shear hinge' ETABS model, this is done based on the performance requirements and compliance criteria set forth in Eurocode 8, part 3. The figure also shows that first yield occurs at the lower beam at a horizontal load of 144.6 KN and at a second story displacement of 4.3 mm which follows a similar pattern to the experiment where lower beam shear cracks were recorded at a load of 148 KN.

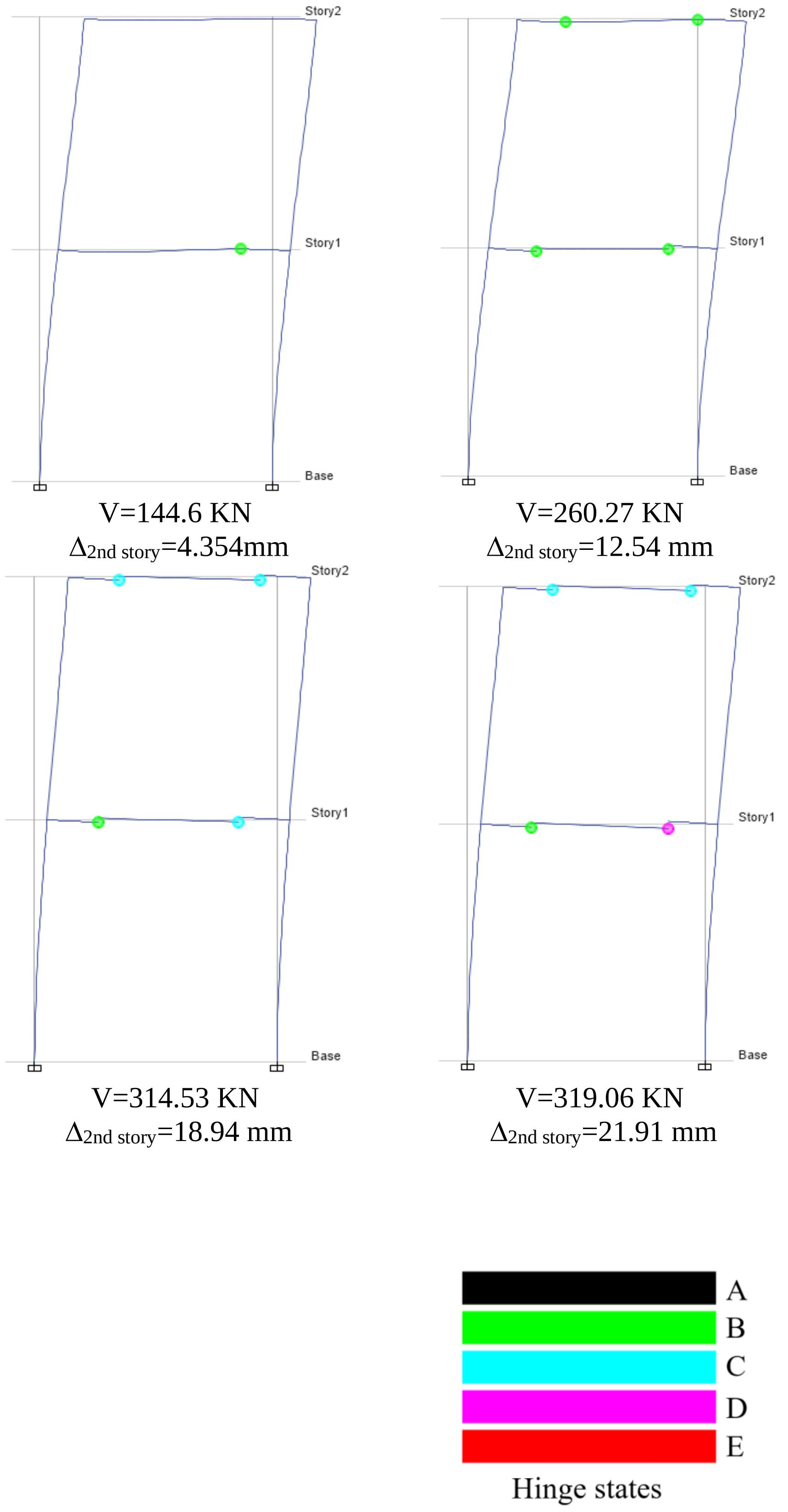

Figure 4-9 Hinge formation of the Doung frame model

CHAPTER 5 CONCLUSIONS AND RECOMMENDATIONS

5.1 Conclusions

In this study the seismic performance of a shear critical frame was investigated through finite element analysis using ETABS, Seismostruct and Vector 2. After the analyses the results were examined using experimental data from a laboratory test carried by Kien Vinh Duong, Shamim A. Sheikh, and Frank J. Vecchio at the University of Toronto. The accuracy of various finite element software in predicting shear critical behavior was scrutinized. Finaly a proposal for steps to be followed to improve the results of one of the most commonly used structural analysis software was set forth, and its out puts verified against experimental data.

First the results from Vector2 model show that the software is more than capable of predicting shear critical behaviour, as indicated by Guner, S., & Vecchio, F. J. (2010). Although the basic version of the software, with limitations on the number of elements and nodes, was used the results were satisfactory. Vector 2 being an educational software developed by one of the top leading institutes when it comes to the study of shear effects in reinforced concrete, its accuracy is expected.

The second model done on SeismoStruct; a software specifically designed for performance assessment of structures was also highly accurate. SeismoStruct being a commercial software it required less effort and user expertise on shear critical behavior making it easily applicable by the standard practitioner.

Next in the modelling done on one of the most widely used structural analysis software, ETABS, using various approaches. The commonly used approach of assuming ductile failure and using only moment hinges resulted in a highly misleading result. This further substantiates the need to carefully consider shear behaviour in the performance assessment of structures built to older codes.

The use of ‘default hinges’ was also examined to see how much improvement it can bring. While this improved the result from the previous ‘no shear hinge’ approach, it still resulted in a significantly higher strength prediction of the frame when compared to the experimental results. This was a misleading overestimation that could have serious consequence if used by a user with limited expertise or lacking in meticulous attention to details.

Finally, user defined shear hinges were used in the 'custom shear hinges' approach. While this required a prior understanding of possible shear mechanism, considerable effort for even a smaller frame size and the use of a speciality supportive software Response 2000, its result was satisfactory. This model showed great convergence to the experimental data when predicting global strength of the specimen. While there is still significant discrepancy in predicting the frame displacement at peak load.

These results show the difficulties in seismic performance assessment of shear critical structures, which led to this thesis study. It is shown that while educational and speciality commercial software are needed for the accurate performance assessment of these structures. The widely used software required expert knowledge to predict the possible failure mechanism of the structure before modelling the structure. This indicates that the standard user might get a misleading result if not aware of possible shear critical mechanism.

5.2 Recommendations

This study is not adequate to fully understand the seismic performance assessment of shear critical structures. The author recommends further research on the following points

I. The author strongly advises conducting laboratory experiments because there is still a lot to learn regarding shear critical behavior. Furthermore, the number of tests conducted on shear critical reinforced concrete frames is still verry low.

II. Other factors that could affect shear critical behavior like inadequate reinforcement anchorage and concrete direct strut action should also be studied.

III. When conducting performance assessment of older building it is recommended to use specialty software that do not rely solely on user expertise.

IV. Checks on ductility character of a structure with regard to detailing and design should preside the assumption of ductile failure commonly used in 'moment hinge only' approaches.

V. Commercial software developers should carefully address the gap in predicting shear critical behavior.

REFERENCES

[1] Duong, K. V., Sheikh, S. A., & Vecchio, F. J. (2007). Seismic behavior of Shear-Critical Reinforced Concrete Frame: Experimental Investigation. ACI Structural Journal, 104(3). https://doi.org/10.14359/18620

[2] Guner, S., & Vecchio, F. J. (2010). Pushover Analysis of Shear-Critical Frames: Verification and Application. (2010c). ACI Structural Journal, 107(01). https://doi.org/10.14359/51663390

[3] Guner, S., & Vecchio, F. J. (2010). Pushover Analysis of Shear-Critical Frames: Formulation. ACI Structural Journal, 107(01). https://doi.org/10.14359/51663389

[4] Guner, S., & Vecchio, F. J. (2011). Analysis of Shear-Critical Reinforced Concrete Plane Frame Elements under Cyclic Loading. Journal of Structural Engineering, 137(8), 834–843. https://doi.org/10.1061/(asce)st.1943-541x.0000346

[5] Acevedo A.B, Bonett-Diaz R.L & Carmona O. (2012). Experimental Analysis of the Lateral Resistance of a Shear Critical Reinforced Concrete Frame. http://hdl.handle.net/10784/29265

[6] Guner, S. (2009b). Performance assessment of shear-critical reinforced concrete plane frames. https://tspace.library.utoronto.ca/handle/1807/16730

[7] F. J. Vecchio and S. Balopoulou. 1990. On the nonlinear behaviour of reinforced concrete frames. *Canadian Journal of Civil Engineering*. **17**(5): 698-704. https://doi.org/10.1139/l90-083

[8] Taucer, F., Spacone, E. & Filippou, F. C. (1991). A fiber beam-column element for seismic response analysis of reinforced concrete structures.

[9] Krawinkler, H., & Seneviratna, G. (1998). Pros and cons of a pushover analysis of seismic performance evaluation. Engineering Structures, 20(4–6), 452–464. https://doi.org/10.1016/s0141-0296(97)00092-8

[10] FEMA (2013). Prestandard and commentary for the seismic rehabilitation of buildings: FEMA 356.

[11] Berhanemeskel Engliz (2015). Performance Assessment of Reinforced Concrete Planar Frame Using Nonlinear Analysis

[12] Satish Paudel & Bikram Bhusal (2020) Investigation of Modelling Approaches for Non-Linear Analysis of Reinforced Concrete Frames

[13] Filippou, F. C., & Issa, A. (1988). Nonlinear analysis of reinforced concrete frames under cyclic load reversals.

[14] Charkhchi, P., Mullapudi, T. R. S., & Ayoub, A. (2010). Fiber beam formulation for analysis of Shear-Critical reinforced concrete shear walls. Structures Congress 2010. https://doi.org/10.1061/41130(369)316

[15] Zhang, Y. P., Diao, B., & Ye, Y. H. (2011). Nonlinear Analytical model of RC Shear-Critical frame elements. Applied Mechanics and Materials, 137, 134–139. https://doi.org/10.4028/www.scientific.net/amm.137.134

[16] Vecchio, F. J., & Collins, M. P. (1986). The Modified Compression-Field theory for reinforced concrete elements subjected to shear. ACI Journal Proceedings, 83(2). https://doi.org/10.14359/10416

[17] Vecchio, F. J. (2000). Disturbed Stress Field Model for Reinforced Concrete: Formulation. Journal of Structural Engineering, 126(9), 1070–1077. https://doi.org/10.1061/(asce)0733-9445(2000)126:9(1070

[18] Mander, J. B., Priestley, M. J. N., & Park, R. (1988). Theoretical Stress-Strain model for confined concrete. Journal of Structural Engineering, 114(8), 1804–1826. https://doi.org/10.1061/(asce)0733-9445(1988)114:8(1804

[19] Inel, M., & Ozmen, H. B. (2006). Effects of plastic hinge properties in nonlinear analysis of reinforced concrete buildings. Engineering Structures, 28(11), 1494–1502. https://doi.org/10.1016/j.engstruct.2006.01.017

[20] ESA (2015). ES EN1998:2015: Design of Structures for Earthquake Resistance Part 1: General Rules, Seismic Actions and Rules for Buildings.

[21] E. Standard Committee (2004). EuroCode 2: Design of Concrete Structures: Part 1-1: General Rules and Rules for Buildings.

[22] E. Standard Committee (2005). EuroCode 8: Design of structures for earthquake resistance - Part 1: General rules, seismic actions and rules for buildings.

[23] E. Standard Committee (2005). EuroCode 8: Design of Structures for Earthquake Resistance - Part 3: Assessment and Retrofitting of Buildings.

[24] CSI (2017). CSI Analysis Reference Manual For SAP2000®, ETABS®, SAFE® and CSiBridge®.

[25] P. S. Wong, F.J. Vecchio & H. Trommels (2013). VECTOR2 & FORMWORKS USER'S MANUAL

[26] Seismosoft Ltd. (2024). SeismoStruct User Manual

[27] Byrne, P. M., Finn, W. D. L., & Ventura, C. E. (1996). The Hyogo-ken Nanbu (Kobe) earthquake of 17 January 1995: seismological aspects and ground motions. Canadian Journal of Civil Engineering, 23(3), 771–777. https://doi.org/10.1139/l96-887

APPENDIX A

A.1 Hand Calculation of Shear capacity for section AA (Beam)

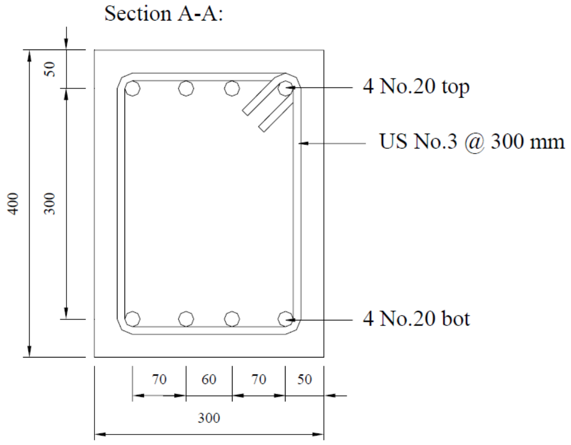

$$f_{ck} = 42Mpa$$
$$b = 300mm$$
$$h = 400mm$$
$$d = 400 - 30 - 9.5 - (19.5/2) = 350.75$$

The shear resistance of members without shear reinforcement $V_{Rd,c}$ is given in *EN1992-1-1 §6.2.2(1), equations (6.2.a) and (6.2.b)*

$$V_{Rd,c} = [C_{Rd,c} K (100\delta_1 f_{ck})^{1/3} + K_1 \sigma_{cp}] b_w d$$

with a minimum of

$$V_{Rd,c} = (v_{\min} + K_1 \sigma_{cp}) b_w d$$

The coefficient $C_{Rd,c}$ is equal to

$$C_{Rd,c} = 0.18/\gamma_c = 0.18/0.15 = 0.12$$

The coefficient k depends on the static depth of the cross-section d (in mm):

$$K = 1 + \sqrt{\frac{200}{d}} = 1 + \sqrt{\frac{200}{350}} = 1.755 \leq 2$$

The percentage of longitudinal reinforcement ρ_l that contributes to the shear strength is defined as follows:

$$\delta_1 = \frac{A_{s1}}{b_w d} = \frac{1200}{300 * 350} = 0.0114 \leq 0.02$$

The coefficient k_1 is equal to $k_1 = 0.150$

The contribution of the axial stress due to loading or prestressing σ_{cp} is limited to:

$$\sigma_{cp} = \frac{N_{Ed}}{A_c} = 0 \leq 0.2 f_{cd}$$

Then $V_{Rd,c}$ becomes

$$\begin{aligned} V_{Rd,c} &= [C_{Rd,c} K (100\delta_1 f_{ck})^{1/3} + K_1 \sigma_{cp}] b_w d \\ &= [0.12 * 1.755 * (100 * 0.0114 * 42.9)^{1/3} + 0.15(0)] 300(350) \\ &= 81.04 KN \end{aligned}$$

The coefficient v_{min} is given by *EN1992-1-1 equation (6.3N)*:

$$v_{\min} = 0.035 K^{3/2} f_{ck}{}^{1/2} = 0.035(1.755)^{3/2}(42.9)^{1/2} = 0.5329$$

The minimum $V_{Rd,c}$ becomes

$$V_{Rd,c} = (v_{\min} + K_1 \sigma_{cp}) b_w d = 0.5329(300)(350) = 56.08 KN$$

The shear resistance of the member without shear reinforcement $V_{Rd,c}$ is obtained from the maximum of the two *equations (6.2.a) and (6.2.b)*

$$V_{Rd,c} = \max[81.04, 56.08] = 81.04 KN$$

The shear resistance of members with shear reinforcement $V_{Rd,s}$ is given in *EN1992-1-1 §6.2.3(3), equation (6.8)*

$$V_{Rd,s} = \frac{A_{sw}}{s} z f_{ywd} Cot\theta$$

With a maximum of $V_{Rd,max}$ corresponding to the resistance of the concrete compression struts

$$V_{Rd,\max} = \alpha_{cw} b_w z v_1 f_{cd} \big/ \cot\theta + \tan\theta$$

The limits on the cotangent cotθ of the angle θ between the concrete compression strut and the beam axis perpendicular to the shear force are specified in *EN 1992-1-1 §6.2.3(2)*

$$1 \leq Cot\theta \leq 2.5$$

Taking a assumption of cot θ=2.5 corresponding to the minimum angle for shear 21.8°

$$V_{Rd,s} = \frac{A_{sw}}{s} z f_{ywd} Cot\theta = \frac{2*71}{300}(0.9*350)(506)(2.5) = 189KN$$

Checking our assumption of cotθ=2.5

$$\theta = 0.5\sin^{-1}\left(\frac{V_{Rd}}{0.2 f_{ck}(1-\frac{f_{ck}}{250})}\right)$$

$$= 0.5\sin^{-1}\left(\frac{189}{0.2(42.9)(1-\frac{42.9}{250})}\right) = 7.32^0 < 21.8^0 \Rightarrow Ok!$$

A.2 Hand Calculation of Shear capacity for section BB (Column)

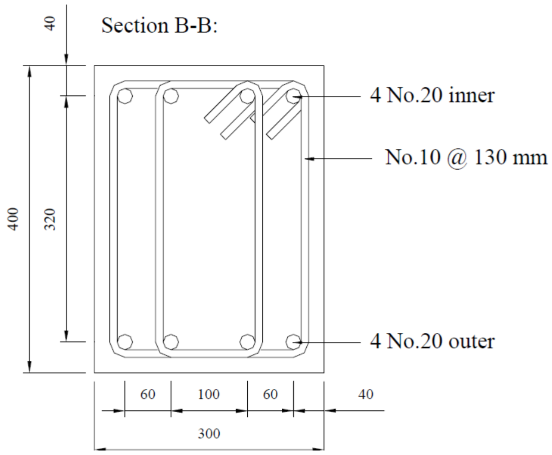

$f_{ck} = 42Mpa$

$b = 300mm$

$h = 400mm$

$d = 400 - 20 - 11.3 - (19.5/2) = 359.1$

The shear resistance of members without shear re

1 §6.2.2(1), equations (6.2.a) and (6.2.b)

$$V_{Rd,c} = [C_{Rd,c} K (100\delta_1 f_{ck})^{1/3} + K_1 \sigma_{cp}] b_w d$$

with a minimum of

$$V_{Rd,c} = (v_{\min} + K_1 \sigma_{cp}) b_w d$$

The coefficient $C_{Rd,c}$ is equal to

$$C_{Rd,c} = 0.18/\gamma_c = 0.18/0.15 = 0.12$$

The coefficient k depends on the static depth of the cross-section d (in mm):

$$K = 1 + \sqrt{\frac{200}{d}} = 1 + \sqrt{\frac{200}{359}} = 1.74 \leq 2$$

The percentage of longitudinal reinforcement ρ_l that contributes to the shear strength is defined as follows:

$$\delta_1 = \frac{A_{s1}}{b_w d} = \frac{1200}{300 * 359} = 0.0114 \leq 0.02$$

The coefficient k_1 is equal to $k_1 = 0.150$

The contribution of the axial stress due to loading or prestressing σ_{cp} is limited to:

$$\sigma_{cp} = \frac{N_{Ed}}{A_c} = \frac{420000}{400*300} = 3.5 \leq (0.2 f_{cd} = 0.2*28.33 = 5.67)$$

Then $V_{Rd,c}$ becomes

$$\begin{aligned} V_{Rd,c} &= [C_{Rd,c}K(100\delta_1 f_{ck})^{1/3} + K_1\sigma_{cp}]b_w d \\ &= [0.12*1.74*(100*0.011*42.9)^{1/3} + 0.15(3.5)]300(359) \\ &= 137.8KN \end{aligned}$$

The coefficient $v_{\min}$ is given by *EN1992-1-1 equation (6.3N)*:

$$v_{\min} = 0.035K^{3/2} f_{ck}^{\ 1/2} = 0.035(1.74)^{3/2}(42.9)^{1/2} = 0.5261$$

The minimum $V_{Rd,c}$ becomes

$$V_{Rd,c} = (v_{\min} + K_1\sigma_{cp})b_w d = (0.5329 + (0.15*3.5))(300)(350) = 111KN$$

The shear resistance of the member without shear reinforcement $V_{Rd,c}$ is obtained from the maximum of the two *equations (6.2.a) and (6.2.b)*

$$V_{Rd,c} = \max[137.8, 111] = 137.8KN$$

The shear resistance of members with shear reinforcement $V_{Rd,s}$ is given in *EN1992-1-1 §6.2.3(3), equation (6.8)*

$$V_{Rd,s} = \frac{A_{sw}}{s} z f_{ywd} Cot\theta$$

With a maximum of $V_{Rd,max}$ corresponding to the resistance of the concrete compression struts

$$V_{Rd,\max} = \alpha_{cw} b_w z v_1 f_{cd} \Big/ \cot\theta + \tan\theta$$

The limits on the cotangent cotθ of the angle θ between the concrete compression strut and the beam axis perpendicular to the shear force are specified in *EN 1992-1-1 §6.2.3(2)*

$$1 \le Cot\theta \le 2.5$$

Several iteration were used to find the value of cot θ, leading to an assumption of cot θ=1.5 corresponding to the minimum angle for shear 21.8°

$$V_{Rd,s} = \frac{A_{sw}}{s} z f_{ywd} Cot\theta = \frac{4*100}{130}(0.9*359)(455)(1.58) = 714KN$$

Checking our assumption of cotθ=1.5

$$\theta = 0.5\sin^{-1}\left(\frac{V_{Rd}}{0.2 f_{ck}(1-\frac{f_{ck}}{250})}\right)$$

$$= 0.5\sin^{-1}\left(\frac{714}{0.2(42.9)(1-\frac{42.9}{250})}\right) = 34.5^0, \cot(34.5^0) = 1.45 \approx 1.5Ok!$$

APPENDIX B

B.1 Base Shear vs Monitored Displacement for ETABS model with no shear hinge

TABLE: Base Shear vs Monitored Displacement

Step	Monitored Displ.	Base Force	A-B	B-C	C-D	D-E	>E	A-IO	IO-LS	LS-CP	>CP	Total
0	0	0	12	0	0	0	0	12	0	0	0	12
1	1.505	50	12	0	0	0	0	12	0	0	0	12
2	3.009	100	12	0	0	0	0	12	0	0	0	12
3	4.515	150	12	0	0	0	0	12	0	0	0	12
4	6.042	200	12	0	0	0	0	12	0	0	0	12
5	7.598	250	12	0	0	0	0	12	0	0	0	12
6	7.876	258.8722	10	2	0	0	0	12	0	0	0	12
7	11.147	308.8722	10	2	0	0	0	12	0	0	0	12
8	12.566	330.4804	8	4	0	0	0	12	0	0	0	12
9	22.395	380.4804	7	5	0	0	0	12	0	0	0	12
10	29.983	406.7178	6	6	0	0	0	11	1	0	0	12
11	32.811	413.2026	5	7	0	0	0	11	1	0	0	12
12	32.833	413.3402	5	7	0	0	0	11	1	0	0	12
13	32.881	413.4733	5	7	0	0	0	11	1	0	0	12
14	32.876	407.2233	5	7	0	0	0	11	1	0	0	12
15	32.991	408.7939	5	7	0	0	0	11	1	0	0	12
16	35.377	413.4783	5	7	0	0	0	9	3	0	0	12
17	50.003	438.4783	5	5	2	0	0	5	5	2	0	12
18	72.9	461.5099	4	4	2	2	0	4	5	1	2	12
19	72.376	443.4463	4	4	2	2	0	4	4	2	2	12
20	70.855	393.4463	4	4	2	2	0	4	4	2	2	12
21	69.334	343.4463	4	4	2	2	0	4	4	2	2	12
22	67.813	293.4463	4	4	2	2	0	4	4	2	2	12
23	66.293	243.4463	4	4	2	2	0	4	4	2	2	12
24	64.756	193.4463	4	4	2	2	0	4	4	2	2	12
25	64.128	172.8659	4	4	1	3	0	4	4	2	2	12
26	66.195	224.7014	4	4	1	3	0	4	4	2	2	12

B.2 Base Shear vs Monitored Displ. for ETABS model with default shear hinge

TABLE: Base Shear vs Monitored Displacement

Step	Monitored Displ.	Base Force	A-B	B-C	C-D	D-E	>E	A-IO	IO-LS	LS-CP	>CP	Total
0	0	0	16	0	0	0	0	16	0	0	0	16
1	1.505	50	16	0	0	0	0	16	0	0	0	16
2	3.009	100	16	0	0	0	0	16	0	0	0	16
3	4.515	150	16	0	0	0	0	14	2	0	0	16
4	6.042	200	16	0	0	0	0	14	2	0	0	16
5	7.598	250	16	0	0	0	0	12	2	2	0	16
6	7.876	258.872	14	2	0	0	0	12	2	2	0	16
7	11.147	308.872	14	2	0	0	0	12	0	4	0	16
8	12.566	330.480	12	4	0	0	0	12	0	4	0	16
9	22.395	380.480	11	5	0	0	0	12	0	4	0	16
10	29.915	406.718	10	6	0	0	0	11	1	4	0	16
11	31.796	409.843	9	7	0	0	0	11	1	4	0	16
12	32.892	412.968	9	7	0	0	0	11	1	4	0	16
13	32.894	413.047	9	7	0	0	0	11	1	4	0	16
14	32.908	412.888	9	7	0	0	0	11	1	4	0	16
15	32.909	412.891	9	7	0	0	0	11	1	4	0	16
16	33.35	410.341	9	7	0	0	0	11	1	4	0	16
17	34.731	413.052	9	7	0	0	0	11	1	4	0	16
18	62.862	453.845	8	6	1	1	0	5	5	5	1	16
19	62.002	422.731	6	6	1	1	2	5	5	3	3	16
20	60.429	372.731	6	6	1	1	2	5	5	3	3	16
21	58.857	322.731	6	6	1	1	2	5	5	3	3	16
22	57.284	272.731	6	6	1	1	2	5	5	3	3	16
23	55.712	222.731	6	6	1	1	2	5	5	3	3	16
24	54.209	174.919	6	6	1	1	2	5	5	3	3	16
25	53.962	171.152	6	6	1	1	2	5	5	3	3	16

B.3 Base Shear vs Monitored Displ. for ETABS model with custom shear hinge 1st iteration

TABLE: Base Shear vs Monitored Displacement

Step	Monitored Displ.	Base Force	A-B	B-C	C-D	D-E	>E	A-IO	IO-LS	LS-CP	>CP	Total
0	0	0	16	0	0	0	0	16	0	0	0	16
1	1.505	50	16	0	0	0	0	16	0	0	0	16
2	3.009	100	16	0	0	0	0	16	0	0	0	16
3	4.515	150	16	0	0	0	0	16	0	0	0	16
4	6.042	200	16	0	0	0	0	16	0	0	0	16
5	7.489	246.51	15	1	0	0	0	16	0	0	0	16
6	12.02	310.74	14	1	1	0	0	16	0	0	0	16
7	14.091	314.96	14	0	2	0	0	16	0	0	0	16
8	17.12	337.49	13	1	2	0	0	16	0	0	0	16
9	19.089	346.73	12	2	2	0	0	16	0	0	0	16

B.4 Base Shear vs Monitored Displ. for ETABS model with custom shear hinge 2nd iteration

TABLE: Base Shear vs Monitored Displacement

Step	Monitored Displ.	Base Force	A-B	B-C	C-D	D-E	>E	A-IO	IO-LS	LS-CP	>CP	Total
0	0	0	16	0	0	0	0	16	0	0	0	16
1	1.505	50	16	0	0	0	0	16	0	0	0	16
2	3.009	100	16	0	0	0	0	16	0	0	0	16
3	4.354	144.6459	15	1	0	0	0	16	0	0	0	16
4	7.4	202.8324	13	3	0	0	0	16	0	0	0	16
5	12.541	260.2699	12	4	0	0	0	16	0	0	0	16
6	18.946	314.5259	12	1	3	0	0	14	2	0	0	16
7	21.913	320.0922	12	1	2	1	0	14	1	0	1	16
8	21.914	319.0639	12	1	2	1	0	14	1	0	1	16
9	20.904	285.327	12	1	2	1	0	14	1	0	1	16
10	19.909	251.7659	12	1	2	1	0	14	1	0	1	16